The Abdus Salam
International Centre
for Theoretical Physics

2512-5

Fundamentals of Ocean Climate Modelling at Global and Regional Scales (Hyderabad - India)

5 - 14 August 2013

Ocean Circulation Models and Modeling

GRIFFIES Stephen

Princeton University
U.S. Department of Commerce N.O.A.A., Geophysical Fluid Dynamics Laboratory, 201 Forrestal Road, Forrestal Campus
P.O. Box 308, 08542-6649 Princeton NJ
U.S.A.

5.1: Ocean Circulation Models and Modeling

Stephen.Griffies@noaa.gov
NOAA/Geophysical Fluid Dynamics Laboratory
Princeton, USA

Anne.Marie.Treguier@ifremer.fr
Laboratoire de Physique des Océans, LPO
Brest, France

Draft from May 24, 2013

5.1.1. Scope of this chapter

We focus in this chapter on numerical models used to understand and predict large-scale ocean circulation, such as the circulation comprising basin and global scales. It is organized according to two themes, which we consider the "pillars" of numerical oceanography. The first addresses physical and numerical topics forming a foundation for ocean models. We focus here on the science of ocean models, in which we ask questions about fundamental processes and develop the mathematical equations for ocean thermo-hydrodynamics. We also touch upon various methods used to represent the continuum ocean fluid with a discrete computer model, raising such topics as the finite volume formulation of the ocean equations; the choice for vertical coordinate; the complementary issues related to horizontal gridding; and the pervasive questions of subgrid scale parameterizations. The second theme of this chapter concerns the applications of ocean models, in particular how to design an experiment and how to analyze results. This material forms the basis for ocean modeling, with the aim being to mechanistically describe, interpret, understand, and predict emergent features of the simulated, and ultimately the observed, ocean.

5.1.2. Physical and numerical basis for ocean models

As depicted in Figure 5.1.1, the ocean experiences a wide variety of boundary interactions and possesses numerous internal physical processes. Kinematic constraints on the fluid motion are set by the geometry of the ocean domain, and by assuming each fluid parcel conserves mass, save for the introduction of mass across the ocean surface (i.e., precipitation, evaporation, river runoff), or bottom (e.g., crustal vents). Dynamical interactions are described by Newton's Laws, in which the acceleration of a continuum fluid parcel is set by forces acting on the parcel. The dominant forces in the ocean interior are associated with pressure, the Coriolis force, gravity, and to a lesser degree friction. Boundary forces arise from interactions with the atmosphere, cryosphere, and solid earth, with each interaction generally involving buoyancy and momentum exchanges. Material budgets for tracers, such as salt and biogeochemical species, as well as thermodynamic tracers such as heat or enthalpy, are affected by circulation, mixing from turbulent processes, surface and bottom boundary fluxes, and internal sources and sinks especially for biologeochemical tracers (see Chapter 5.7).

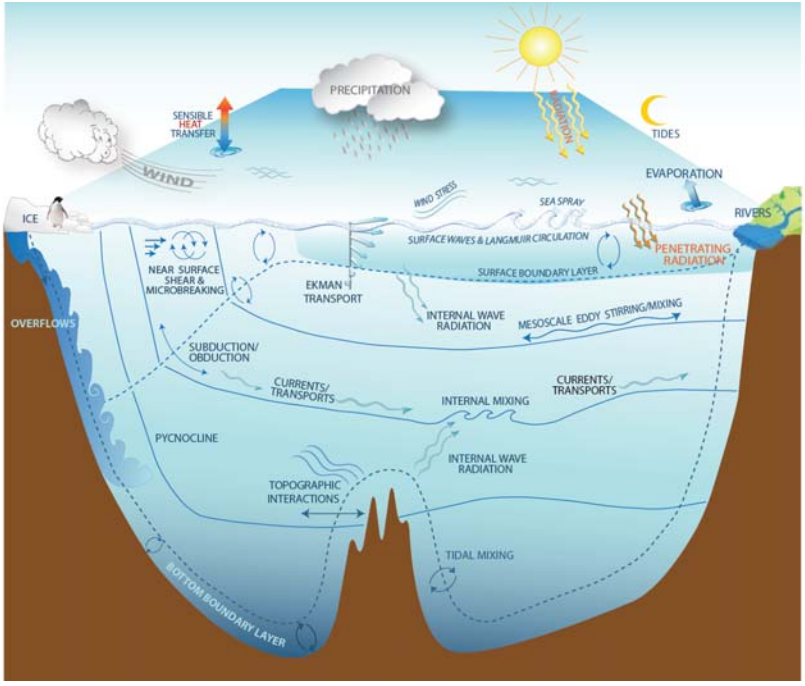

Figure 5.1.1: Understanding and quantifying the ocean's role in the earth system, including coastal, regional, and global phenomena, involves a variety of questions related to how physical processes impact the movement of tracers (e.g., heat, salt, carbon, nutrients) and momentum across the ocean boundaries and within the ocean interior. The ocean interacts with the variety of earth system components, including the atmoshere, sea ice, land ice shelves, rivers, and the solid earth lower boundary. Ocean processes transport material between the ventilated surface boundary layer and the ocean interior. When in the interior, it is useful to characterize processes according to whether they transport material across density surface (dianeutrally) or along neutral directions (epineutrally). In this figure we illustrate the turbulent air-sea exchanges and upper ocean wave motions (including wave breaking and Langmuir circulations); subduction/obduction which exchanges material between the boundary layer and interior; gyre-scale, mesoscale, and submesoscale transport that largely occurs along neutral directions; high latitude convective and downslope exchange; and mixing induced by breaking internal gravity waves energized by winds and tides. Missing from this schematic include mixing due to double diffusive processes (Schmitt (1994)) and nonlinear equation of state effects (Chapter 3.2). Nearly all such processes are subgrid scale for present day global ocean climate simulations. The formulation of sensible parameterizations, including schemes that remain relevant under a changing climate (e.g., modifications to stratification and boundary forcing), remains a key focus of oceanographic research efforts, with Chapters 3.3 and 3.4 in this volume detailing many issues.

5.1.2.1. Scales of motion

The ocean's horizontal gyre and overturning circulations occupy nearly the full extent of ocean basins (10^3 km to 10^4 km in horizontal extent and roughly 4 km in depth on average), with typical recirculation times for the horizontal gyres of decadal, and overturning time scales of millennial. The ocean microscale is on the order of 10^{-3} m, and it is here that mechanical energy is transferred to internal energy through

Joule heating. The microscale is set by the *Kolmogorov length*

$$L_{\text{Kol}} = (\nu^3/\epsilon)^{1/4}, \tag{5.1.1}$$

where $\nu \approx 10^{-6}\ \text{m}^2\ \text{s}^{-1}$ is the molecular kinematic viscosity for water, and ϵ is the energy dissipation rate. In turn, molecular viscosity and the Kolmogorov length imply a time scale $T = L^2/\nu \approx 1$ sec.

Consider a direct numerical simulation of ocean climate, where all space and time scales between the Kolmogorov scale and the global scale are explicitly resolved by the simulation. One second temporal resolution over a millennial time scale climate problem requires more than 3×10^{10} time steps of the model equations. Resolving space into cubes of dimension 10^{-3}m for an ocean with volume roughly $1.3 \times 10^{18}\ \text{m}^3$ requires 1.3×10^{27} discrete grid cells, which is roughly 10^4 larger than Avogadro's Number. These numbers far exceed the capacity of any computer, thus necessitating approximated or truncated descriptions for practical ocean simulations, and furthermore promoting the central importance of subgrid scale parameterizations.

5.1.2.2. Thermo-hydrodynamic equations for a fluid parcel

As a starting point for developing ocean model equations, we consider the thermo-hydrodynamic equations for an infinitesimal seawater parcel. Some of this material is standard from geophysical fluid dynamics as applied to the ocean (e.g., see books such as Gill (1982), Pedlosky (1987), Vallis (2006), Olbers et al. (2012)), so the presentation here will be focused on setting the stage for later discussions.

Mass conservation for seawater and trace constituents

When formulating the tracer and dynamical equations for seawater, it is convenient to focus on a fluid parcel whose mass is constant. Writing the mass as $M = \rho\, \mathrm{d}V$, with $\mathrm{d}V$ the parcel's infinitesimal volume and ρ the *in situ* density, parcel mass conservation $\mathrm{d}M/\mathrm{d}t = 0$ yields the continuity equation

$$\frac{\mathrm{d}\rho}{\mathrm{d}t} = -\rho\, \nabla \cdot \mathbf{v}. \tag{5.1.2}$$

The three-dimensional velocity of the parcel is the time derivative of its position, $\mathbf{v} = \mathrm{d}\mathbf{x}/\mathrm{d}t$, and the horizontal and vertical components are written $\mathbf{v} = (\mathbf{u}, w)$. Transforming this parcel or material Lagrangian expression into a fixed space or Eulerian perspective leads to the equivalent form

$$\frac{\partial \rho}{\partial t} = -\nabla \cdot (\rho\, \mathbf{v}), \tag{5.1.3}$$

where we related the material time derivative to the Eulerian time derivative through

$$\frac{\mathrm{d}}{\mathrm{d}t} = \partial_t + \mathbf{v} \cdot \nabla. \tag{5.1.4}$$

Seawater is comprised of fresh water along with a suite of matter constituents such as salt, nutrients, and biogeochemical elements and compounds. The tracer concentration, C, which is the mass of trace matter within a seawater parcel per mass of the parcel, is affected through the convergence of a tracer flux plus a potentially nonzero source/sink term $\mathcal{S}^{(C)}$ (sources and sinks are especially important for describing biogeochemical tracers; Chapter 5.7)

$$\rho \frac{\mathrm{d}C}{\mathrm{d}t} = -\nabla \cdot \mathbf{J}^{(\mathrm{c})} + \rho\, \mathcal{S}^{(C)}. \tag{5.1.5}$$

The canonical form of the tracer flux is associated with isotropic downgradient molecular diffusion

$$\mathbf{J}^{(\mathrm{c})}_{\text{molecular}} = -\rho\, \kappa\, \nabla C, \tag{5.1.6}$$

where $\kappa > 0$ is a kinematic molecular diffusivity with units of length times a velocity, and $\rho\, \kappa$ is the corresponding dynamic diffusivity. For large-scale ocean models, the tracer flux $\mathbf{J}^{(\mathrm{c})}$ is modified according to the parameterization of various unresolved physical processes (see Chapters 3.3 and 3.4).

The Eulerian perspective converts the material time derivative into a local Eulerian time derivative plus advection $\rho\, (\partial_t + \mathbf{v} \cdot \nabla)\, C = -\nabla \cdot \mathbf{J}^{(\mathrm{c})} + \rho\, \mathcal{S}^{(C)}$. Combining this advective-form tracer equation with the seawater mass equation (5.1.3) leads to the Eulerian flux-form of the tracer equation

$$\partial_t\, (\rho\, C) = -\nabla \cdot (\rho\, \mathbf{v}\, C + \mathbf{J}^{(\mathrm{C})}) + \rho\, \mathcal{S}^{(C)}. \tag{5.1.7}$$

Setting the tracer concentration to a uniform constant in the tracer equation (5.1.7) recovers the mass continuity equation (5.1.3), where we assumed there to be no seawater mass source, and the tracer flux $\mathbf{J}^{(\mathrm{c})}$ vanishes with the concentration constant (e.g., see Section II.2 of DeGroot & Mazur (1984), Section 8.4 of Chaikin & Lubensky (1995), or Section 3.3 of Müller (2006)). This connection between the tracer equation and the seawater mass continuity equation is sometimes referred to as a *compatibility condition* (see Griffies et al. (2001) or Chapter 12 of Griffies (2004)). Equivalently, requiring that the tracer equation maintain a uniform tracer unchanged in the absence of boundary fluxes is sometimes referred to as *local* tracer conservation, which is a property required for conservative numerical algorithms. The flux-form in equation (5.1.7) is used in Section 5.1.2.4 as the basis for developing finite volume equations for a region of seawater.

Conservative temperature and *in situ* density

As detailed by McDougall (2003), potential enthalpy provides a useful measure of heat in a seawater parcel (see also Chapter 3.2). Conservative temperature, Θ, is the potential enthalpy divided by a constant heat capacity. According to the First Law of Thermodynamics, it satisfies, to an extremely good approximation, a scalar conservation equation directly analogous to material tracers

$$\rho \frac{\mathrm{d}\Theta}{\mathrm{d}t} = -\nabla \cdot \mathbf{J}^{(\Theta)}. \tag{5.1.8}$$

This equation, or its Eulerian form, are termed "conservative" since the net heat content in a region is impacted only through fluxes passing across the boundary of that region (see Chapter 5.7 for more discussion of conservative and non-conservative tracers).

In fact, there are actually nonzero source terms that are neglected in equation (5.1.8), so that conservative temperature is not precisely "conservative". However, McDougall (2003) noted that these omitted source terms are negligible, as they are about 100 times smaller than those source terms omitted when considering potential temperature, θ, to be a conservative scalar. It is for this reason that IOC et al. (2010) recommend the use of conservative temperature, Θ, as a means to measure the heat of a seawater parcel.

The equation of state, which provides an empirical expression for the *in situ* density ρ, is written as a function of conservative temperature, salinity, and pressure

$$\rho = \rho(\Theta, S, p). \tag{5.1.9}$$

Note that the equation of state as derived in IOC et al. (2010) is written in terms of the Gibb's thermodynamic potential, thus making it self-consistent with other thermodynamic properties of seawater. Based on this connection, efforts are underway to update ocean model codes and analysis methods towards the recommendations of IOC et al. (2010).

Momentum equation

Newton's Second Law of Motion applied to a continuum fluid in a rotating frame of reference leads to the equation describing the evolution of linear momentum per volume of a fluid parcel

$$\rho \left(\frac{\mathrm{d}}{\mathrm{d}t} + 2\,\boldsymbol{\Omega} \wedge \right) \mathbf{v} = -\rho\,\nabla\Phi + \nabla \cdot (\boldsymbol{\tau} - \mathbf{I}\,p). \tag{5.1.10}$$

The momentum equation (5.1.10) encapsulates nearly all the phenomena of ocean and atmospheric fluid mechanics. Such wide applicability is a testament to the power of classical mechanics to describe observed natural phenomena. The terms in the equation are the following.

- Acceleration: When considering fluid dynamics on a flat space, the acceleration times density, $\rho\,\mathrm{d}\mathbf{v}/\mathrm{d}t$, takes the following Eulerian flux-form

  $$\rho \frac{\mathrm{d}\mathbf{v}}{\mathrm{d}t} = \frac{\partial\,(\rho\,\mathbf{v})}{\partial t} + \nabla \cdot (\rho\,\mathbf{v}\,\mathbf{v}) \qquad \text{flat space}, \tag{5.1.11}$$

  which is directly analogous to the flux-form tracer equation (5.1.7). However, for fluid dynamics on a curved surface such as a sphere, the acceleration picks up an extra source-like term that is associated with curvature of the surface. When using locally orthogonal coordinates to describe the motion, acceleration takes the form (see Section 4.4.1 of Griffies (2004))

  $$\rho \frac{\mathrm{d}\mathbf{v}}{\mathrm{d}t} = \frac{\partial\,(\rho\,\mathbf{v})}{\partial t} + \nabla \cdot (\rho\,\mathbf{v}\,\mathbf{v}) + \mathcal{M}\,(\hat{\mathbf{z}} \wedge \rho\,\mathbf{v}) \qquad \text{sphere}. \tag{5.1.12}$$

  For spherical coordinates, $\mathcal{M} = (u/r)\,\tan\phi$, with ϕ the latitude and r the radial position. At latitude $\phi = 45°$ with $r \approx 6.37 \times 10^6$m, and for a zonal current of $u = 1$ m s^{-1}, $\mathcal{M} \approx 10^{-3} f$, where

  $$f = 2\,\Omega\,\sin\phi \tag{5.1.13}$$

is the Coriolis parameter (see below). Hence, $\mathcal{M}$ is generally far smaller than the inertial frequency, f, determined by the Earth's rotation, except near the equator where f vanishes.

The nonlinear self-advective transport term $\rho\,\mathbf{v}\,\mathbf{v}$ contributing to the acceleration (see equation (5.1.12)) accounts for the rich variety of nonlinear and cross-scale turbulent processes that pervade the ocean. At the small scales (hundreds of metres and smaller), such processes increase three-dimensional gradients of tracer and velocity through straining and filamentation effects, and in so doing increase diffusive fluxes. In turn, tracer variance and kinetic energy cascade to the small scales through the effects of three-dimensional turbulence (*direct cascade*), and are dissipated at the microscale (millimetres) by molecular viscosity and diffusivity. At the larger scales where vertical stratification and quasi-geostrophic dynamics dominates (Chapter 4.1), kinetic energy preferentially cascades to the large scales (*inverse cascade*) as in two-dimensional fluid dynamics, whereas tracer variance continues to preferentially cascade to the small scales. Such cascade processes are fundamental to how energy and tracer variance are transferred across the many space-time scales within the ocean fluid.

- Coriolis force: Angular rotation of the earth about the polar axis, measured by $\boldsymbol{\Omega}$, leads to the Coriolis force per volume, $2\,\rho\,\boldsymbol{\Omega}\,\wedge\,\mathbf{v}$. The locally horizontal component to the rotation vector, $f^{*} = 2\,\Omega\,\cos\phi$, can induce *tilted convection* that causes convecting plumes to deflect laterally (Denbo & Skyllingstad (1996), Wirth & Barnier (2006, 2008)). Another effect was noted by Stewart & Dellar (2011), who argue for the importance of f^{*} in cross-equatorial flow of abyssal currents. However, hydrostatic primitive equation ocean models, which are the most common basis for large-scale models of the ocean, retain only the local vertical component of the earth's rotation, and thus approximate the Coriolis Force according to

$$2\,\rho\,\boldsymbol{\Omega}\,\wedge\,\mathbf{v} \approx \hat{\mathbf{z}}\,f\,\wedge\,(\rho\,\mathbf{v}), \tag{5.1.14}$$

  where f (equation (5.1.13)) is termed the Coriolis parameter. Marshall et al. (1997) provides a discussion of this approximation and its connection to hydrostatic balance. It is this form of the Coriolis force that gives rise to many of the characteristic features of geophysical fluid motions, such as Rossby waves, Kelvin waves, western boundary currents, and other large-scale features (Chapter 4.1).

- Gravitational force: The gravitational potential, Φ, is commonly approximated in global circulation models as a constant gravitational acceleration, g, times the displacement, z, from resting sea level or the surface ocean geopotential (geoid),

$$\Phi \approx g\,z. \tag{5.1.15}$$

  However, the geopotential must be considered in its more general form when including astronomical tide forcing and/or changes to the geoid due to rearrangements of mass; e.g., melting land ice such as in the studies of Mitrovica et al. (2001) and Kopp et al. (2010).

- Frictional stresses and pressure: The symmetric second order deviatoric stress tensor, $\boldsymbol{\tau}$, accounts for the transfer of momentum between fluid parcels due to shears, whereas p is the pressure force acting normal to the boundary of the parcel, with $\mathbf{I}$ the unit second order tensor. At the microscale, frictional stresses are parameterized by molecular diffusive fluxes in the same way as for tracers in equation (5.1.6), with this parameterization based on analogy with the kinetic theory of gases (e.g., section 12.3 of Reif (1965)). Vertical stresses in the ocean interior are thought to be reasonably well parameterized in this manner for large-scale ocean models, with the eddy viscosity far larger than molecular viscosity due to momentum mixing by unresolved eddy processes. In contrast, there is no consensus on how to represent lateral frictional stress in large-scale ocean models, with modelers choosing lateral friction based on empirical (i.e., "tuning") perspectives (Part 5 in Griffies (2004), as well as Jochum et al. (2008) and Fox-Kemper & Menemenlis (2008) for further discussion). In Section 5.1.2.6, we have more to say about certain issues involved with setting lateral friction in models.

Comments on the parcel equations

The mass conservation equation (5.1.2), tracer equation (5.1.5), conservative temperature equation (5.1.8), equation of state (5.1.9), momentum equation (5.1.10), and boundary conditions (Section 5.1.2.4), are the basic building blocks for a mathematical physics description of ocean thermo-hydrodynamics. However, these equations alone do not provide an algorithm for numerical simulations. Indeed, we know of no algorithm, much less a working numerical code, based on a realistic nonlinear equation of state for a mass conserving and non-hydrostatic ocean. Instead, various approximations are made, either together or separately, that have proven useful for developing numerical ocean model algorithms.

5.1.2.3. Approximation methods

Three general approaches to approximation, or truncation, are employed in computational fluid dynamics, and we outline here these approaches as used for ocean models.

Coarse grid and realistic large-scale domain

One approach is to coarsen the space and time resolution used by the discrete grid forming the basis for the numerical simulation. By removing scales smaller than the grid, the truncated system carries less information than the continuum. Determining how the resolved scales are affected by the unresolved scales is fundamental to the science of ocean models: this is the parameterization problem (Section 5.1.2.5).

Refined grid and idealized small domain

A complementary approach is to configure a small space-time domain so as to maintain the very fine space and time resolution set by either molecular viscosity and diffusivity (direct numerical simulation (DNS)), or somewhat larger eddy viscosity and diffusivity (large eddy simulation (LES)). These simulations are necessarily idealized both because of their small domain and the associated need to include idealized boundary conditions. Both DNS and LES are important for process studies aimed at understanding the mechanisms active in fine scale features of the ocean. Insights gained via DNS and LES have direct application to the development of subgrid scale parameterizations used in large-scale models. Large-scale simulations that represent a wide range of mesoscale and submesoscale eddies (e.g., finer than 1 km grid spacing) share much in common with LES (Fox-Kemper & Menemenlis, 2008). Such simulations will conceivably be more common for global climate scales within the next one or two decades, as computational power increases.

Filtering the continuum equations: hydrostatic approximation

A third truncation method filters the continuum equations by truncating the fundamental modes of motion admitted by the equations. This approach reduces the admitted motions and reduces the space-time scales required to simulate the system.

The hydrostatic approximation is a prime example of mode filtering used in large-scale modeling. Here, the admitted vertical motions possess far less kinetic energy than horizontal motions, thus rendering a simplified vertical momentum balance where the weight of fluid above a point in the ocean determines the pressure at that point

$$\frac{\partial p}{\partial z} = -\rho \, \frac{\partial \Phi}{\partial z} \qquad \text{hydrostatic balance.} \tag{5.1.16}$$

Since vertical convective motion involves fundamentally non-hydrostatic dynamics (Marshall & Schott, 1999), hydrostatic primitive equation models must parameterize these effects (Klinger et al., 1996). Although the hydrostatic approximation is ubiquitous in large scale ocean modeling (for scales larger than roughly 1 km), there are many process studies that retain non-hydrostatic dynamics, with the MIT general circulation model (MITgcm) a common publicly available code used for such studies (Marshall et al., 1997).

Filtering the continuum equations: oceanic Boussinesq approximation

In situ density in the large-scale ocean varies by a relatively small amount, with a 5% variation over the full ocean column mostly due to compressibility. Furthermore, the dynamically relevent horizontal density variations are on the order of 0.1%. These observations motivate the *oceanic Boussinesq approximation*.

As detailed in Section 9.3 of Griffies & Adcroft (2008), the first step to the oceanic Boussinesq approximation applies a linearization to the momentum equation by removing the nonlinear product of density times velocity, in which the product $\rho \, \mathbf{v}$ is replaced by $\rho_o \, \mathbf{v}$, where ρ_o is a constant Boussinesq reference density. However, one retains the *in situ* density dependence of the gravitational potential energy, and correspondingly it is retained for computing pressure. The second step considers the mass continuity equation (5.1.3), where the three-dimensional flow is incompressible to leading order

$$\nabla \cdot \mathbf{v} = 0 \qquad \text{volume conserving Boussinesq approximation.} \tag{5.1.17}$$

This step filters acoustic modes (i.e., sound waves), if they are not already filtered by making the hydrostatic approximation.

As revealed by the mass conservation equation (5.1.2), a nontrivial material evolution of *in situ* density requires a divergent velocity field. However, a divergent velocity field is unresolved in oceanic Boussinesq models. Not resolving the divergent velocity field does not imply this velocity vanishes. Indeed, the oceanic Boussinesq approximation retains the dependence of density on pressure (or depth), temperature, and salinity (equation (5.1.9)), thus avoiding any assumption regarding the fluid properties. In turn, such models allow for a consistent material evolution of *in situ* density, with this evolution critical for representing the thermohaline induced variations in density (and hence pressure) that are key drivers of the large scale ocean circulation (Chapter 4.1).

An element missing from Boussinesq ocean models concerns the calculation of global mean sea level. Greatbatch (1994) noted that the accumulation of seawater compressibility effects over an ocean column leads to meaningful systematic changes in global sea level when, for example, the ocean is heated. These global steric effects must therefore be added *a posteriori* to a Boussinesq simulation of sea level to provide a meaningful measure of global sea level changes associated with buoyancy forcing (see also the sea level discussion in Chapter 6.1). Griffies & Greatbatch (2012) build on the work of Greatbatch (1994) by detailing how physical processes impact global mean sea level in ocean models.

5.1.2.4. Thermo-hydrodynamic equations for a finite region

Our next step in developing the equations of an ocean model involves integrating the continuum parcel equations over a finite region, with the region boundaries generally moving and permeable. The resulting budget equations form the basis for a finite volume discretization of the ocean equations. They may also be used to develop basin-wide budgets for purposes of large-scale analysis (Section 5.1.3.2). The finite volume approach serves our pedagogical aims, and it forms the basis for most ocean models in use today for large-scale studies. We make reference to the schematic shown in Figure 5.1.2 relevant for a numerical model.

Finite volume budget for scalars and momentum

Consider a volume of fluid, V, with a moving and permeable boundary $\mathcal{S}$. The tracer mass budget within this region satisfies

$$\frac{\partial}{\partial t}\left(\int_V C\,\rho\,\mathrm{d}V\right) = -\int_{\mathcal{S}} \hat{\mathbf{n}}\cdot[(\mathbf{v}-\mathbf{v}^{\mathcal{S}})\,\rho\,C + \mathbf{J}]\,\mathrm{d}\mathcal{S}, \tag{5.1.18}$$

where we ignored tracer source/sink terms for brevity, dropped the superscript (C) on the subgrid scale tracer flux $\mathbf{J}$, and wrote $\hat{\mathbf{n}}$ for the outward normal to the boundary. Tracer mass within a region (left hand side) changes due to the passage of tracer through the boundary, either from advective transport or subgrid scale transport (right hand side). Advective transport is measured according to the normal projection of the fluid velocity in a frame moving with the surface, $\mathbf{v}-\mathbf{v}^{\mathcal{S}}$. The subgrid scale tracer transport must likewise be measured relative to the moving surface. The finite volume budget for seawater mass is obtained by setting the tracer concentration to a constant in the tracer budget (5.1.18)

$$\frac{\partial}{\partial t}\left(\int_V \rho\,\mathrm{d}V\right) = -\int_{\mathcal{S}} \hat{\mathbf{n}}\cdot(\mathbf{v}-\mathbf{v}^{\mathcal{S}})\,\rho\,\mathrm{d}\mathcal{S}. \tag{5.1.19}$$

The relation between the mass budget (5.1.19) and tracer budget (5.1.18) is a manifestation of the compatibility condition discussed following the continuum tracer equation (5.1.7). An analogous finite volume budget follows for the hydrostatic primitive equations, in which we consider the horizontal momentum over a finite region with the Coriolis Force in its simplified form (5.1.14)

$$\begin{aligned} \partial_t \left(\int_V \mathbf{u}\,\rho\,\mathrm{d}V \right) &= - \int_V [\, g\,\hat{\mathbf{z}} + (f + \mathcal{M})\,\hat{\mathbf{z}} \wedge \mathbf{u}]\,\rho\,\mathrm{d}V \\ &\quad - \int_{\mathcal{S}} [\,\hat{\mathbf{n}} \cdot (\mathbf{v} - \mathbf{v}^{\mathcal{S}})]\,\mathbf{u}\,\rho\,\mathrm{d}\mathcal{S} + \int_{\mathcal{S}} \hat{\mathbf{n}} \cdot (\boldsymbol{\tau} - \mathbf{I}\,p)\,\mathrm{d}\mathcal{S}. \end{aligned} \tag{5.1.20}$$

The volume integral on the right hand side arises from the gravitational and Coriolis body forces, whereas the surface integrals arise from both advective transport and contact forces associated with stress and pressure.

Some domain boundaries are static, such as the lateral boundaries for a model grid cell or the solid earth boundaries of an ocean basin (Figure 5.1.2). However, vertical boundaries are quite often moving, with the ocean free surface

$$z = \eta(x, y, t) \tag{5.1.21}$$

a canonical example. In this case, the projection of the boundary velocity onto the normal direction is directly proportional to the time tendency of the free surface

$$\hat{\mathbf{n}} \cdot \mathbf{v}^{\mathcal{S}} = \left(\frac{\partial \eta}{\partial t} \right) |\nabla\,(z - \eta)|^{-1}. \tag{5.1.22}$$

Iso-surfaces of a generalized vertical coordinate

$$s = s(x, y, z, t) \tag{5.1.23}$$

are generally space and time dependent. For example, the grid cell top and bottom may be bounded by surfaces of constant pressure, potential density, or another moving surface. Here, the normal component of the surface velocity is proportional to the tendency of the generalized vertical coordinate

$$\hat{\mathbf{n}} \cdot \mathbf{v}^{\mathcal{S}} = - \left(\frac{\partial s}{\partial t} \right) |\nabla\,s|^{-1}. \tag{5.1.24}$$

Generalized vertical coordinates and dia-surface transport

To make use of a finite volume budget for layers defined by generalized vertical coordinates requires that the vertical coordinate be monotonically stacked in the vertical, so that there is a one-to-one relation between the geopotential coordinate, z, and the generalized vertical coordinate. Mathematically, this constraint means that the *specific thickness* $\partial s/\partial z$ never vanishes, and thus remains of one sign throughout the domain so there are no inversions in the generalized vertical coordinate iso-surfaces. An important case where $\partial s/\partial z = 0$ occurs for isopycnal models in regions of zero vertical density stratification. Handling such regions necessitates either a transformation to a stably stratified vertical coordinate such as pressure, as in the Hybrid Ocean Model

(HYCOM) code of Bleck (2002), or appending a bulk mixed layer (Hallberg, 2003) to the interior isopycnal layers as in the Miami Isopycnal Coordinate Ocean Model (MICOM) code of Bleck (1998), or the General Ocean Layer Dynamics (GOLD) code used in Adcroft et al. (2010).

The monotonic assumption (i.e., $\partial s/\partial z$ remains single signed) allows us to measure the advective transport across the constant s surfaces according to the dia-surface velocity component (Section 2.2 of Griffies & Adcroft (2008))

$$\rho\, w^{(s)} \equiv \frac{(\textsc{mass/time})\ \textsc{of fluid thru surface}}{\textsc{area of horiz projection of surface}} \tag{5.1.25a}$$

$$= \frac{\hat{\mathbf{n}} \cdot (\mathbf{v} - \mathbf{v}^{S})\, \rho\, \mathrm{d}\mathcal{S}}{\mathrm{d}A}, \tag{5.1.25b}$$

where $\mathrm{d}A$ is the horizontal projection of the surface area $\mathrm{d}\mathcal{S}$. Questions of how to measure dia-surface mass transport arise in many areas of ocean model formulation as well as construction of budgets for ocean domains. We present here two equivalent expressions

$$w^{(s)} = \left(\frac{\partial z}{\partial s}\right) \frac{\mathrm{d}s}{\mathrm{d}t} \tag{5.1.26a}$$

$$= w - (\partial_t + \mathbf{u} \cdot \nabla_s)\, z, \tag{5.1.26b}$$

in which $\nabla_s z = -(\partial z/\partial s)\, \nabla_z s$ is the slope of the s surface as projected onto the horizontal plane (Chapter 6 of Griffies (2004)). Equation (5.1.26a) indicates that if the vertical coordinate has zero material time derivative, then there is zero dia-surface mass transport. Equation (5.1.26b) is commonly encountered when studying subduction of water from the mixed layer to the ocean interior, in which the generalized vertical coordinate is typically an isopycnal or isotherm (e.g., Marshall et al. (1999)). A final example of dia-surface transport arises from motion across the ocean free surface at $z = \eta(x, y, t)$, in which case

$$Q_{\mathrm{m}}\, \mathrm{d}A \equiv (\textsc{mass/time})\ \textsc{of fluid through free surface} \tag{5.1.27a}$$

$$= -\mathrm{d}A\, (w - \mathbf{u} \cdot \nabla\eta - \partial_t \eta)\, \rho, \tag{5.1.27b}$$

with $Q_{\mathrm{m}} > 0$ if mass enters the ocean. Rearrangement leads to the surface kinematic boundary condition

$$\rho\, (\partial_t + \mathbf{u} \cdot \nabla)\, \eta = w + Q_{\mathrm{m}} \qquad \text{at } \ z = \eta. \tag{5.1.28}$$

Surface and bottom boundary conditions

The tracer flux leaving the ocean through the free surface is given by (see equation (5.1.18))

$$\int\limits_{z=\eta} \hat{\mathbf{n}} \cdot [(\mathbf{v} - \mathbf{v}^{S})\, \rho\, C + \mathbf{J}]\, \mathrm{d}\mathcal{S} = \int\limits_{z=\eta} (-Q_{\mathrm{m}}\, C + J^{(s)})\, \mathrm{d}A, \tag{5.1.29}$$

where

$$\mathrm{d}A\, J^{(s)} = \mathrm{d}\mathcal{S}\, \hat{\mathbf{n}} \cdot \mathbf{J} \tag{5.1.30}$$

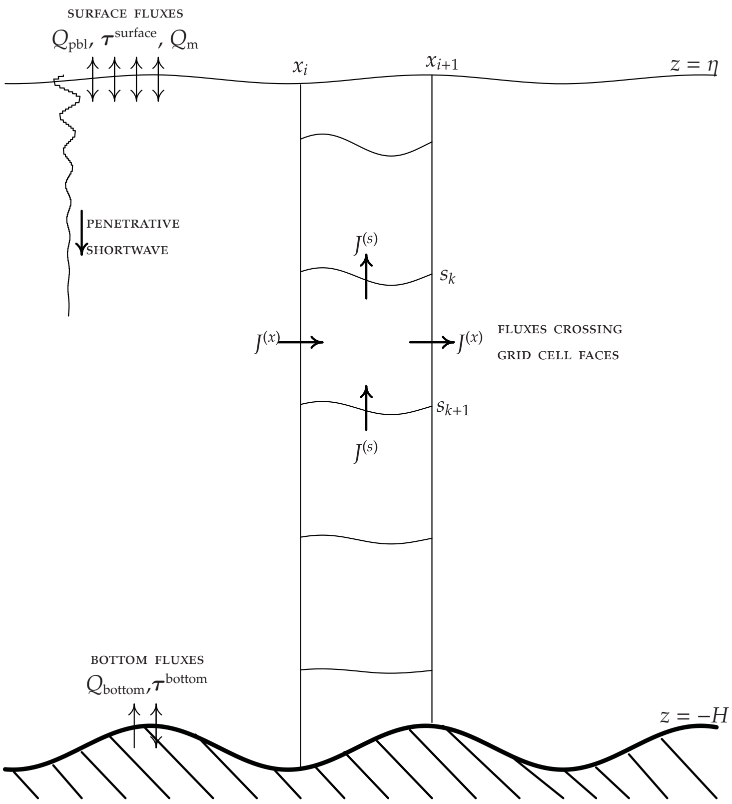

Figure 5.1.2: A longitudinal-vertical slice of ocean fluid from the surface at $z = \eta(x, y, t)$ to bottom at $z = -H(x, y)$, along with a representative column of discrete grid cells (a latitudinal-vertical slice is analogous). Most ocean models used for large-scale climate studies assume the horizontal boundaries of a grid cell at x_i amd x_{i+1} are static, whereas the vertical extent, defined by surfaces of constant generalized vertical coordinate s_k and s_{k+1}, can be time dependent. The tracer flux $\mathbf{J}$ is decomposed into horizontal and dia-surface components, with the convergence of these fluxes onto a grid cell determining the evolution of tracer content within the cell. Similar decomposition occurs for momentum fluxes. Additional terms contributing to the evolution of tracer include source terms, and momentum evolution also includes body forces (Coriolis and gravity). Amongst the fluxes crossing the ocean surface, the shortwave flux penetrates into the ocean column as a function of the optical properties of seawater (e.g., Manizza et al., 2005).

is the dia-surface tracer transport associated with subgrid scale processes and/or parameterized turbulent boundary fluxes. Boundary fluxes are often given in terms of bulk formula (see, e.g., Taylor (2000), Appendix C of Griffies et al. (2009), and Section 5.1.3.1), allowing for the boundary flux to be written in the form

$$-\int_{z=\eta} \hat{\mathbf{n}} \cdot [(\mathbf{v} - \mathbf{v}^{\mathcal{S}})\, \rho\, C + \mathbf{J}]\, \mathrm{d}\mathcal{S} = \int_{z=\eta} (Q_{\text{m}}\, C_{\text{m}} + Q_{\text{pbl}})\, \mathrm{d}A, \qquad (5.1.31)$$

where C_{m} is the tracer concentration within the incoming mass flux Q_{m}. The first term on the right hand side of equation (5.1.31) represents the advective transport of tracer through the surface with the water (i.e., ice melt, rivers, precipitation, evaporation). The term Q_{pbl} arises from parameterized turbulence and/or radiative fluxes within the surface planetary boundary layer, such as sensible, latent, shortwave, and longwave heating as occurs for the temperature equation, with $Q_{\mathrm{pbl}} > 0$ signaling tracer entering the ocean through its surface. A similar expression to (5.1.31) holds at the ocean bottom $z = -H(x, y)$, though it is common in climate modeling to only consider geothermal heating (Adcroft et al., 2001; Emile-Geay & Madec, 2009) with zero mass flux.

The force acting on the bottom surface of the ocean is given by

$$\mathbf{F}_{\text{bottom}} = -\int\limits_{z=-H} [\,\nabla(z+H)\cdot\boldsymbol{\tau} - p\,\nabla(z+H)]\,\mathrm{d}A. \tag{5.1.32}$$

In the presence of a nonzero topography gradient, $\nabla H \neq 0$, the term $-p\,\nabla H$ at the ocean bottom gives rise to a topographic *form stress* that affects horizontal momentum. Such stress is especially important for strong flows that reach to the ocean bottom, such as in the Southern Ocean (Chapter 4.8). Parameterization of this stress is particularly important for models that only resolve a coarse-grained representation of topography. In addition to form stress, we assume that a boundary layer model, typically in the form of a drag law, provides information so that we can parameterize the bottom vector stress

$$\boldsymbol{\tau}^{\text{bottom}} \equiv \nabla(z+H)\cdot\boldsymbol{\tau} \qquad \text{at } z = -H \tag{5.1.33}$$

associated with bottom boundary layer momentum exchange. This parameterization of bottom stress necessarily incorporates interactions between the ocean fluid with small scale topography variations, so that there is a non-zero vector stress $\boldsymbol{\tau}^{\text{bottom}}$ even if the large-scale topography resolved by a numerical model is flat. Additional considerations for the interactions between unresolved mesoscale eddies with topography lead to the Neptune parameterization of Holloway (1986, 1989, 1992).

Momentum transfer through the ocean surface is given by

$$\mathbf{F}_{\text{surface}} = \int\limits_{z=\eta} [\,\boldsymbol{\tau}^{\text{surface}} - p_{\mathrm{a}}\,\nabla\,(z-\eta) + Q_{\mathrm{m}}\,\mathbf{u}_{\mathrm{m}}]\,\mathrm{d}A. \tag{5.1.34}$$

In this equation, $\mathbf{u}_{\mathrm{m}}$ is the horizontal velocity of the mass transferred across the ocean boundary. This velocity is typically taken equal to the velocity of the ocean currents in the top cell of the ocean model, but such is not necessarily the case when considering the different velocities of, say, river water and precipitation. The vector stress

$$\boldsymbol{\tau}^{\text{surface}} \equiv \nabla\,(z-\eta)\cdot\boldsymbol{\tau} \qquad \text{at } z = \eta \tag{5.1.35}$$

arises from the wind, as well as interactions between the ocean and ice. As for the bottom stress parameterization (5.1.33), a boundary layer model determining the surface vector stress, $\boldsymbol{\tau}^{\text{surface}}$, must consider subgrid-scale fluctuations of the sea surface, such as nonlinear effects associated with surface waves (Sullivan & McWilliams, 2010; Cavaleri et al., 2012; Belcher et al., 2012). Finally, we take the applied pressure at $z = \eta$ to equal the pressure p_a from the media sitting above the ocean; namely, the atmosphere and ice. As for the bottom force, there is generally a nonzero horizontal projection of the applied pressure acting on the curved free surface, $p_a \nabla \eta$, thus contributing to an applied surface pressure form stress on the ocean.

5.1.2.5. Physical considerations for transport

Working with a discrete rather than continuous fluid presents many fundamental and practical issues. One involves the introduction of unphysical *computational modes* whose presence can corrupt the simulation; e.g., dispersion arising from discrete advection operators can lead to spurious mixing (Griffies et al. (2000b), Ilicak et al. (2012)). Another issue involves the finite grid size, Δ, or more generally the finite degrees of freedom available to simulate a continuum fluid. The grid scale is generally many orders larger than the Kolmogorov scale (equation (5.1.1))

$$\Delta \gg L_{\text{Kol}}, \tag{5.1.36}$$

and Δ determines the degree to which an oceanic flow feature can be resolved by a simulation.

There are two reasons to parameterize a physical process impacting the ocean. The first is if the process is filtered from the continuum equations forming the basis for the model, such as the hydrostatic approximation (5.1.16). The second concerns the finite grid scale. To understand how the grid introduces a closure or parameterization problem, consider a *Reynolds decomposition* of an advective flux

$$\overline{u\,\psi} = \overline{u}\,\overline{\psi} + \overline{u'\,\psi'}, \tag{5.1.37}$$

where $u = \overline{u} + u'$ expresses a velocity component as the sum of a mean and fluctuation, and the average of a fluctuating field is assumed to vanish, $\overline{u'} = 0$. The same decomposition is assumed for the field being transported, ψ, which could be a tracer concentration or velocity component. The discrete grid represents the product of the averaged fields, $\overline{u}\,\overline{\psi}$, through a numerical advection operator. Computing this resolved transport using numerical methods is the *representation problem*, which involves specification of a numerical advection operator. The correlation term, $\overline{u'\,\psi'}$, is not explicitly represented on the grid, with its specification constituting the *subgrid scale parameterization problem*. The correlation term is referred to as a *Reynolds stress* if ψ is a velocity component, and an *eddy flux* if ψ is a tracer. To deduce information about the second order correlation $\overline{u'\,\psi'}$ requires third order correlations, which are functions of fourth order correlations, etc., thus forming the *turbulence closure problem*. Each process depicted in Figure 5.1.1 contributes to fluctuations, so they each engender a closure problem if unresolved.

The theory required to produce *mean field* or averaged fluid equations is extensive and nontrivial. A common aim is to render the resulting subgrid scale correlations in a form subject to physical insight and sensible parameterization. The variety of averaging methods amount to different mathematical approaches that are appropriate under differing physical regimes and are functions of the vertical coordinates used to describe the fluid. A non-exhaustive list of examples specific to the ocean include the following (see also Olbers et al. (2012) for further discussion of even more averaging methods).

- The microscale or infra-grid averaging of DeSzoeke & Bennett (1993), Davis (1994a), Davis (1994b), and DeSzoeke (2009) focuses on scales smaller than a few tens of metres.

- The density weighted averaging of Hesselberg (1926) (see also McDougall et al. (2002) and Chapter 8 of Griffies (2004)), provides a framework to account for the mass conserving character of the non-Boussinesq ocean equations, either hydrostatic or non-hydrostatic.

- The isopycnal thickness weighted methods of DeSzoeke & Bennett (1993), McDougall & McIntosh (2001), DeSzoeke (2009), and Young (2012) (see also Chapter 9 of Griffies (2004)) provide a framework to develop parameterizations of mesoscale eddy motions in the stratified ocean interior; see also the combined density and thickness weighted methods of Greatbatch & McDougall (2003). Eden et al. (2007) propose an alternative that averages over the same mesoscale phenomena, but maintains an Eulerian perspective rather than moving to isopycnal space.

There are few robust, and even fewer first principle, approaches to parameterization, with simulations often quite sensitive to the theoretical formulation as well as specific details of the numerical implementation. One may choose to ignore the topic of parameterizations, invoking an *implicit large eddy simulation* (ILES) philosophy (Margolin et al. (2006), Grinstein et al. (2007), Shchepetkin & McWilliams (1998)), whereby the responsibility for closing the transport terms rests on the numerical methods used to represent advection. For large-scale modeling, especially with applications to climate, this approach is not common since the models are far from resolving many of the known important dynamical scales, such as the mesoscale. However, it is useful to test this approach to expose simulation features where the absence of a parameterization leads to obvious biases. Delworth et al. (2012) provides one such example, in which the ocean model component of a coupled climate model permits, but does not resolve, mesoscale eddies, and yet there is no parameterization of the unresolved portion of the mesoscale eddies. Determining methods of mesoscale parameterization for use in mesoscale eddy permitting models is an active research area. In general, simulations extending over decadal to longer times must confront an ocean whose circulation and associated water masses are fundamentally impacted by the zoo of physical processes depicted in Figure 5.1.1, most of which are unresolved and have nontrivial impacts on the simulation.

Parameterizing transport in a stratified ocean

In an ideal ocean without mixing, tracer concentration is reversibly stirred by the resolved velocity field (Eckart, 1948). That is, tracer concentration is materially constant (equation (5.1.5) with zero right hand side), and all tracer iso-surfaces are impenetrable to the resolved fluid flow. Mixing changes this picture, with molecular diffusion the ultimate cause of mixing and irreversibility. Upon averaging the equations according to the grid scale of a numerical model of a stratified ocean, subgrid eddy tracer fluxes associated with mesoscale eddies are generally parameterized by downgradient diffusion oriented according to neutral directions (Solomon, 1971; Redi, 1982), with this parameterization termed *neutral*, *epineutral*, or *isoneutral* diffusion. As noted by Gent & McWilliams (1990), there is an additional eddy advective flux (see also Gent et al. (1995) and Griffies (1998)). Over the past decade, the use of such *neutral physics* parameterizations has become ubiquitous in ocean climate models since they generally improve simulations of water masses (Chapter 3.4).

Dianeutral processes mix material across neutral directions (Chapter 3.3). These processes arise from enhanced mixing in upper and lower boundary layers (e.g., Large et al. (1994), Legg et al. (2009)), as well as regions above rough topography (Polzin et al. (1997), Toole et al. (1997), Kunze & Sanford (1996), Naveira-Garabato et al. (2004), Kunze et al. (2006), MacKinnon et al. (2010)). Dianeutral mixing in the ocean interior away from rough topography is far smaller (Ledwell et al., 1993, 2011). Additionally, double diffusive processes (salt fingering and diffusive convection) arise from the differing rates for heat and salt diffusion (Schmitt, 1994). Finally, cabbeling and thermobaricity (Chapter 3.2) may play an important role in dianeutral transport within the ocean interior, especially in the Southern Ocean (Marsh (2000), Iudicone et al. (2008), Klocker & McDougall (2010)). Cabbeling and thermobaricity arise from epineutral mixing of temperature and salinity in the presence of the nonlinear equation of state for seawater (McDougall (1987)).

Although vigorous in parts of the ocean, dianeutral transport is extremely small in other parts in comparison to the far larger epineutral transport. Indeed, ocean measurements indicate that the ratio of dianeutral to epineutral transport is roughly 10^{-8} in many regions away from boundaries and above relatively smooth bottom topography (Ledwell et al., 1993, 2011), and it can become even smaller at the equator (Gregg et al., 2003). Although tiny by comparison for much of the ocean, dianeutral transport in the ocean interior is in fact an important process involved with modifying vertical stratification. Consequently, it impacts fundamentally on the ocean's role in climate. In ocean climate models, the parameterization of interior dianeutral mixing has evolved from a prescribed and static vertical diffusivity proposed by Bryan & Lewis (1979), to a collection of subgrid scale processes largely associated with breaking internal gravity waves and other sources of enhanced vertical shear (e.g., Large et al. (1994), Simmons et al. (2004), Jackson et al. (2008), Melet et al. (2013)) (Chapter 3.2).

Two emerging ideas for parameterization

We mention two emerging approaches to account for subgrid scale processes that may impact on ocean climate modeling in the near future. Although much work remains to determine whether either will become practical, there are compelling physical and numerical reasons to give these proposals serious investigation.

Stochastic closure. Hasselmann (1976) noted that certain components of the climate system can be considered a stochastic, or noise, forcing that contributes to the variability of other components. The canonical example is an ocean that transfers the largely white noise fluctuations from the atmospheric weather patterns into a red noise response (i.e., increased power at the low frequencies) (Frankignoul & Hasselmann (1977), Hall & Manabe (1997)). More recently, elements of the atmospheric and climate communities have considered a stochastic term in the numerical model equations used for weather forecasting and climate projections, with particular emphasis on the utility for tropical convection; e.g., see Williams (2005) and Palmer & Williams (2008) for pedagogical discussions. This noise term is meant to parameterize elements of unresolved fluctuations as they feedback onto the resolved fields.

Depending on the phenomena, there are cases where subgrid scale ocean fields are indeed fluctuating chaotically. Furthermore, the averaging operation applied to the nonlinear terms does not generally satisfy the Reynolds assumption of zero average for the fluctuating terms (i.e., $\overline{u'} \neq 0$) (Davis (1994b), DeSzoeke (2009)). So along with the compelling results from atmospheric models, there are reasons to consider introducing a stochastic element to the subgrid scale terms used in an ocean model (Berlov, 2005; Brankart, 2013; Kitsios et al., 2013).

Super-parameterization. In an effort to improve the impact of atmospheric convective processes on the large-scale, Grabowski (2001) embedded a two-dimensional non-hydrostatic model into a three-dimensional large-scale hydrostatic primitive equation model. The non-hydrostatic model feeds information to the hydrostatic model about convective processes, and the hydrostatic model in turn provides information about the large-scale to the non-hydrostatic model. Khairoutdinov et al. (2008) further examined this *super-parameterization* approach and showed some promising results. Campin et al. (2011) in turn have applied the approach to oceanic convection (see Figure 5.1.3). Some processes are perhaps not parameterizable, and so must be explicitly represented. Additionally, some processes are not represented or parameterized well using a particular modeling framework. Both of these cases may lend themselves to super-parameterizations.

We consider a super-parameterization to be the use of a sub-model (or child model) that is two-way embedded into the main or parent-model, with the sub-model focused on representing certain processes that the parent-model either cannot resolve or does a poor job of representing due to limitations of its numerical methods. In this regard, super-parameterization ideas share features with two-way nesting approaches (Debreu & Blayo, 2008), in which a nested fine grid region resolves processes that the coarse grid parent-model cannot (we have more to say on nesting in Section 5.1.3.1). The approach of Bates et al. (2012a,b) is another example, in which a dynamic and interactive three-dimensional Lagrangian sub-model is embedded in an Eulerian model.

Where we stand with physical parameterizations

Many of the same questions regarding parameterizations raised in the review of Griffies et al. (2000a) remain topical in the research community today. This longevity is both a reflection of the difficulty of the associated theoretical and numerical issues, and the importance of developing robust parameterizations suitable for a growing suite of applications. We offer the following assessment regarding the parameterization question:

> A necessary condition for the evaluation of a physical process parameterization in global ocean climate simulations is to examine companion climate simulations that fully resolve the process.

That is, we will not know the physical integrity of a parameterization until the parameterized process is fully resolved. This assessment does not mean that comparisons

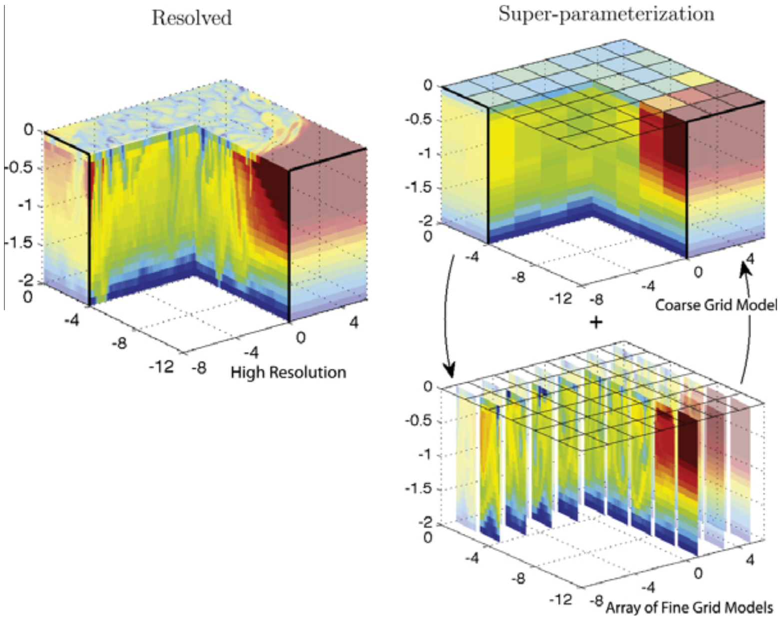

Figure 5.1.3: Three-dimensional view of the temperature field (red is warm, blue is cold) in two simulations of chimney convection similar to Jones & Marshall (1993). Left side: from a high resolution simulation which resolves small scale plume processes. Right side: from a super-parameterized model in which a coarse-grain (CG) large-scale model (top right panel) representing balanced motion is integrated forward with embedded fine-grained (FG) (bottom right panel) running at each column of the large-scale grid. The FG is non-hydrostatic and attempts to resolve the small-scale processes. The FGs and the CG are integrated forward together and exchange information following the algorithm set out in Campin et al. (2011). This figure is based on Figure 1 of Campin et al. (2011).

between models and field observations, laboratory studies, or process studies, are irrelevant to the parameterization question. It does, however, summarize the situation with regard to certain phenomena such as the mesoscale, as supported with recent experience studying the Southern Ocean response to wind stress changes. As shown by Farneti et al. (2010), mesoscale eddying models respond in a manner closer to the observational analysis from Böning et al. (2008) than certain coarse resolution non-eddying models using parameterizations. Prompted by this study, numerous authors have made compelling suggestions for improving the mesoscale eddy parameterizations (e.g., Farneti & Gent (2011), Hofmann & Morales-Maqueda (2011), Gent & Danabasoglu (2011)).

The above assessment does not undermine the ongoing quest to understand processes, such as mesoscale eddy transport, and to develop parameterizations for use in coarse grid models. However, it does lend a degree of humility to those arguing for the validity of their favorite parameterization. It also supports the use of ensembles of model simulations whose members differ by perturbing the physical parameterizations and numerical methods in sensible manners to more fully test the large space of unknown parameters.

5.1.2.6. Numerical considerations for transport

We propose the following as an operational definition for resolution of a flow feature.

> A flow feature is *resolved* only so far as there are no less than 2π grid points spanning the feature.

This definition is based on resolving a linear wave with a discrete, non-spectral, representation so that any admitted wave has length no smaller than $2\pi\,\Delta$. We consider this a sensible operational definition even when representing nonlinear and turbulent motion. Decomposing the flow into vertical baroclinic modes, one is then led to considering the baroclinic flow as resolved only so far as there are 2π grid points for each baroclinic wave whose contribution to the flow energy is nontrivial. Traditionally we write the Rossby radius as $R = 1/\kappa$, with the wavenumber $\kappa = 2\pi/\lambda$ and λ the baroclinic wavelength. Hence, if the grid spacing is less than the Rossby radius, $\Delta \leq R$, then the grid indeed resolves the corresponding baroclinic wave since $2\,\pi\,\Delta \leq \lambda$. As the first baroclinic mode dominates much of the mid-latitude ocean (Wunsch & Stammer (1995), Wunsch (1997), Stammer (1998), Smith & Vallis (2001), Smith (2007)), modelers generally look to the first baroclinic Rossby radius as setting the scale whereby baroclinic flow is resolved (Smith et al. (2000)). Higher baroclinic modes, submesoscale modes (Boccaletti et al. (2007), Fox-Kemper et al. (2008), Klein & Lapeyre (2009)), internal gravity wave modes (Arbic et al., 2010), and other filamentary features require even finer resolution.

Ensuring that admitted flow features are resolved

Nonlinear eddying flows contain waves with many characteristic lengths, and turbulent flows experience an energy and variance cascade between scales (see Section 5.1.2.2 or Vallis (2006)). Furthermore, in the presence of a strongly nonlinear flow, certain discretizations of the nonlinear self-advection term $\rho\,\mathbf{v}\,\mathbf{v}$ (see equation (5.1.12)) can introduce grid scale energy even when the eddying flow is geostrophic and thus subject to the inverse cascade. So quite generally, resolving all flow features admitted in a simulation requires one to minimize the energy and variance contained at scales smaller than $2\pi\Delta$.

There are two general means to dissipate energy and variance of unresolved flow features. The implicit LES approach places responsibility for dissipation with the numerical advection operators acting on momentum and tracer. When coupled to a highly accurate underlying discretization of the advection fluxes, and with a monotonicity constraint that retains physically sensible values for the transport field, such numerical transport operators can be constructed to ensure that only well resolved flow features are admitted. The Regional Ocean Model System (ROMS) (Shchepetkin & McWilliams, 2005) has incorporated elements of this approach, in which lateral friction or diffusion operators are not required for numerical purposes.

The second approach to dissipating unresolved flow features is to incorporate a friction operator into the momentum equation, and diffusion operator into the tracer equation, each using a transport coefficient that is far larger than molecular. There are straightforward ways to do so, yet a naive use of these methods can lead to over-dissipation of the simulation (Griffies & Hallberg (2000), Large et al. (2001), Smith & McWilliams (2003), Jochum (2009)), and/or spurious dianeutral mixing associated with diffusion across density fronts (Veronis (1975), Roberts & Marshall (1998)). Consequently, more sophisticated dissipation operators are typically considered, with their design based on a mix between physical and numerical needs (e.g., see Chapter 14 of Griffies (2004)).

Representing transport in a numerical ocean

The extreme anisotropy between dianeutral and epineutral transport in the ocean interior has motivated the development of ocean models based on potential density as the vertical coordinate (see Section 5.1.2.7). Respecting the epineutral/dianeutral anisotropy in non-isopycnal models is a nontrivial problem in three-dimensional numerical transport. Level models or terrain following models must achieve small levels of spurious dianeutral mixing through a combination of highly accurate tracer advection schemes, and properly chosen momentum and tracer closure schemes, all in the presence of hundreds to thousands of mesoscale eddy turnover times and a nonlinear equation of state.

As noted by Griffies et al. (2000a), resolving all flow features (see Section 5.1.2.6) is difficult for mesoscale eddying simulations, since eddies pump tracer variance to the grid scale and thus increase tracer gradients. At some point, a tracer advection scheme will either produce dispersive errors, and so introduce spurious extrema and thus expose the simulation to spurious convection, or add dissipation via a mixing operator or low order upwind biased advection operator in order to preserve monotonicity.

Methods for reducing spurious dianeutral transport

Mechanical energy cascades to the large scale in a geostrophically turbulent flow. However, grid scale energy can appear as the nonlinear advection of momentum becomes more dominant with eddies, thus stressing the numerical methods used to transport momentum. This issue is directly connected to the spurious dianeutral tracer transport problem, since even very accurate tracer advection schemes, such as the increasingly popular scheme from Prather (1986) (see Maqueda & Holloway (2006), Tatebe & Hasumi (2010), Hill et al. (2012) for ocean model examples) will be exposed to unphysically large spurious transport and/or dispersion error (which produce tracer extrema) if the velocity field contains too much energy (i.e., noise) near the grid scale. Hence, the integrity of momentum transport, and the associated momentum closure, becomes critical for maintaining physically sensible tracer transport, particularly with an eddying flow or any flow where momentum advection is important (Ilicak et al., 2012).

Results from Griffies et al. (2000a), Jochum et al. (2008), and Ilicak et al. (2012) emphasize the need to balance the quest for more kinetic energy, which generally pushes the model closer to observed energy levels seen in satellites (see, e.g., Figure 5.1.4 discussed in Section 5.1.3, or Chapter 2.2), with the need to retain a negligible spurious potential energy source whose impact accumulates over decades and longer.

Following Ilicak et al. (2012), we suggest that maintaining a grid Reynolds number so that

$$\mathrm{Re}_{\Delta} = \frac{U\,\Delta}{\nu} < 2 \tag{5.1.38}$$

ensures unresolved flow features are adequately filtered. In this equation, U is the velocity scale of currents admitted in the simulation, Δ is the grid scale, and ν is the generally non-constant Laplacian eddy viscosity used to dissipate mechanical energy.

The constraint (5.1.38) has multiple origins. One is associated with the balance between advection and diffusion in a second order discretization (see Bryan et al. (1975) or Section 18.1.1 of Griffies (2004)), in which $\mathrm{Re}_{\Delta} < 2$ eliminates an unphysical mode. More recently, Ilicak et al. (2012) identified this constraint as necessary to ensure that spurious dianeutral mixing is minimized. ROMS (Shchepetkin & McWilliams, 2005) has this constraint built into the advection of momentum, whereas most other codes require specification of a friction operator. Selective use of a flow dependent viscosity, such as from a Laplacian or biharmonic Smagorinsky scheme (see Smagorinsky (1993), Griffies & Hallberg (2000), or Section 18.3 of Griffies (2004)), or the scheme of Leith (1996) discussed by Fox-Kemper & Menemenlis (2008), assists in maintaining the constraint (5.1.38) while aiming to avoid over-dissipating kinetic energy in the larger scales.

5.1.2.7. Vertical coordinates

There are three traditional approaches to choosing vertical coordinates: geopotential, terrain-following, and potential density (isopycnal). Work continues within each model class to expand its regimes of applicability, with significant progress occurring in many important areas. The review by Griffies et al. (2010) provides an assessment of recent efforts, which we now summarize.

We start this discussion by noting that all vertical coordinates found to be useful in ocean modeling remain "vertical" in the sense they retain a simple expression for the hydrostatic balance (5.1.16), thus allowing for a hydrostatic balance to be trivially maintained in a simulation. This constraint is a central reason ocean and atmospheric modelers favour the projected non-orthogonal coordinates first introduced by Starr (1945), rather than locally orthogonal coordinates whose form of hydrostatic balance is generally far more complex.

Geopotential and generalized level models

Geopotential z-coordinate models have found wide-spread use in global climate applications for several reasons, such as their simplicity and straightforward nature of parameterizing the surface boundary layer and associated air-sea interaction. For example, of the 25 coupled climate models contributing to the CMIP3 archive used for the IPCC AR4 (Meehl et al., 2007), 22 employ geopotential ocean models, one is terrain-following, one is isopycnal, and one is hybrid pressure-isopycnal-terrain.

There are two key shortcomings ascribed to z-coordinate ocean models.

- Spurious mixing: This issue was discussed in Section 5.1.2.6.

- OVERFLOWS: Downslope flows (Legg, 2012) in z-models tend to possess excessive entrainment (Roberts & Wood (1997),Winton et al. (1998) Legg et al. (2006), Legg et al. (2008), Treguier et al. (2012)), and this behaviour compromises simulations of deep watermasses derived from dense overflows. Despite much effort and progress in understanding both the physics and numerics (Dietrich et al. (1987), Beckmann & Döscher (1997), Beckmann (1998), Price & Yang (1998), Killworth & Edwards (1999), Campin & Goosse (1999), Nakano & Suginohara (2002), Wu et al. (2007), Danabasoglu et al. (2010), Laanaia et al. (2010)), the representation/parameterization of overflows remains difficult at horizontal grid spacing coarser than a few kilometers (Legg et al., 2006).

A shortcoming related to the traditional representation of topography (e.g., Cox (1984)) has largely been overcome by partial cells now commonly used in level models (Adcroft et al. (1997), Pacanowski & Gnanadesikan (1998), Barnier et al. (2006)). It is further reduced by the use of a momentum advection scheme conserving both energy and enstrophy, and by reducing near-bottom sidewall friction (Penduff et al. (2007) and Le Sommer et al. (2009)). A complementary problem arises from the use of free surface geopotential coordinate models, whereby they can lose their surface grid cell in the presence of refined vertical spacing. Generalizations of geopotential coordinates, such as the stretched geopotential coordinate, z^*, introduced by Stacey et al. (1995) and Adcroft & Campin (2004), overcome this problem (see Griffies et al. (2011) and Dunne et al. (2012) for recent global model applications). Leclair & Madec (2011) introduce an extension to z^* that aims to reduce spurious dianeutral mixing. Additional efforts toward mass conserving non-Boussinesq models have been proposed by Huang et al. (2001), DeSzoeke & Samelson (2002) and Marshall et al. (2004), with one motivation being the direct simulation of the global steric effect required for sea level studies (Greatbatch (1994), Griffies & Greatbatch (2012)). What has emerged from the geopotential model community is a movement towards such *generalized level* coordinates that provide enhanced functionality while maintaining essentially the physical parameterizations developed for geopotential models. We thus hypothesize that the decades of experience and continued improvements with numerical methods, parameterizations, and applications suggest that generalized level methods will remain in use for ocean climate studies during the next decade and likely much longer.

Isopycnal layered and hybrid models

Isopycnal models generally perform well in the ocean interior, where flow is dominated by quasi-adiabatic dynamics, as well as in the representation/parameterization of dense overflows (Legg et al., 2006). Their key liability is that resolution is limited in weakly stratified water columns. For ocean climate simulations, isopycnal models attach a non-isopycnal surface layer to describe the surface boundary layer. Progress has been made with such *bulk mixed layer* schemes, so that Ekman driven restratification and diurnal cycling are now well simulated (Hallberg, 2003). Additionally, when parameterizing lateral mixing along constant potential density surfaces rather than neutral directions, isopycnal the models fail to incorporate dianeutral mixing associated with thermobaricity (McDougall, 1987) (see Section A.27 of IOC et al. (2010)). Iudicone et al. (2008) and Klocker & McDougall (2010) suggest that thermobaricity contributes more to water mass transformation in the Southern Ocean than from breaking internal gravity waves.

Hybrid models offer an alternative means to eliminate liabilities of the various traditional vertical coordinate classes. The HYCOM code of Bleck (2002) exploits elements of the hybrid approach, making use of the Arbitrary Lagrangian-Eulerian (ALE) method for vertical remapping (Donea et al., 2004). As noted by Griffies et al. (2010), progress is being made to address issues related to the use of isopcynal layered models, or their hybrid brethren, thus providing a venue for the use of such models for a variety of applications, including global climate (Megann et al. (2010), Dunne et al. (2012)).

A physical system of growing importance for sea level and climate studies concerns the coupling of ocean circulation to ice shelves whose grounding lines can evolve. Required of such models is a land-ocean boundary that evolves, in which case ocean models require a wetting and drying method. We have in mind the growing importance of studies of coupled ice-shelf ocean processes with evolving grounding lines (Goldberg et al., 2012) (see Chapter 4.6 in this volume). Though not uncommon for coastal modeling applications, wetting and drying for ocean climate model codes remain rare, with the study of Goldberg et al. (2012) using the GOLD isopycnal code of Adcroft et al. (2010) the first to our knowledge. It is notable that climate applications require exact conservation of mass and tracer to remain viable for long-term (decadal and longer) simulations, whereas certain of the wetting and drying methods used for coastal applications fail to meet this constraint. We conjecture that isopycnal models, or their generalizations using ALE methods, will be very useful for handling the evolving coastlines required for such studies.

Terrain following vertical coordinate models

Terrain-following coordinate models (TFCM) have found extensive use for coastal and regional applications, where bottom boundary layers and topography are well-resolved. As with geopotential models, TFCMs generally suffer from spurious dianeutral mixing due to problems with numerical advection (Marchesiello et al., 2009). Also, the formulation of neutral diffusion (Redi, 1982) and eddy-induced advection (Gent & McWilliams, 1990) has until recently not been considered for TFCMs. However, recent studies by Lemarié et al. (2012a,b) have proposed new methods to address both of these issues.

A well known problem with TFCMs is calculation of the horizontal pressure gradient, with errors leading to potentially nontrivial spurious flows. Errors are a function of topographic slope and near-bottom stratification (Haney (1991), Deleersnijder & Beckers (1992), Beckmann & Haidvogel (1993), Mellor et al. (1998), and Shchepetkin & McWilliams (2002)). The pressure gradient problem has typically meant that TFCMs are not useful for global-scale climate studies with realistic topography, at least until horizontal grid spacing is very fine (order 10 km or finer). However, Lemarié et al. (2012b), following from Mellor et al. (1998), identify an intriguing connection between pressure gradient errors and the treatment of lateral diffusive transport. Namely, the use of neutral diffusion rather than terrain-following diffusion in grids of order 50 km with the Regional Ocean Model System (ROMS) (Shchepetkin & McWilliams, 2005) significantly reduces the sensitivity of the simulation to the level of topographic

MODEL	VERTICAL COORDINATE	WEB SITE
HYCOM	hybrid $\sigma - \rho - p$	`hycom.org/ocean-prediction`
MIT	general level	`mitgcm.org/`
MOM	general level	`mom-ocean.org`
NEMO	general level	`nemo-ocean.eu/`
POM	terrain following	`aos.princeton.edu/WWWPUBLIC/PROFS/NewPOMPage.html`
POP	geopotential	`climate.lanl.gov/Models/POP/`
ROMS	terrain following	`myroms.org/`

Table 5.1.1: Open source ocean model codes with structured horizontal grids applicable for a variety of studies including large-scale circulation. These codes are currently undergoing active development (i.e., updated algorithms, parameterizations, diagnostics, applications), possess thorough documentation, and maintain widespread community support and use. Listed are the model names, vertical coordinate features, and web site where code and documentation are available. We failed to find other model codes that satisfy these criteria.
Each model is coded in Fortran with generalized orthogonal horizontal coordinates. MOM and POP use an Arakawa B-grid layout of the discrete momentum equations, whereas others use an Arakawa C-grid (see Griffies et al. (2000a) for a summary of B and C grids). General level models are based on the traditional z-coordinate approach, but may be generalized to include other vertical coordinates such as pressure or terrain following. HYCOM's vertical coordinate algorithm is based on vertical remapping to return coordinate surfaces at each time step to their pre-defined targets. In contrast, general level models diagnose the dia-surface velocity component through the continuity equation (Adcroft & Hallberg, 2006), which is the fundamental distinction from general layered or quasi-Lagrangian models such as HYCOM.
Acronyms are the following: HYCOM = Hybrid Coordinate Ocean Model, MIT = Massachusetts Institute of Technology, MOM = Modular Ocean Model, NEMO = Nucleus for European Modelling of the Ocean, POM = Princeton Ocean Model, POP = Parallel Ocean Progran, ROMS = Regional Ocean Modeling System.

smoothing. This result suggests that it is not just the horizontal pressure gradient error that has plagued terrain following models, but the additional interaction between numerically-induced mixing of active tracers and the pressure gradient.

Where we stand with vertical coordinates

Table 5.1.1 provides a list of open source codes maintaining an active development process, providing updated and thorough documentation, and supporting an international user community. There are fewer codes listed in Table 5.1.1 than in the Griffies et al. (2000a) review written at the close of the WOCE era. It is inevitable that certain codes will not continue to be widely supported. There has also been a notable merger of efforts, such as in Europe where the majority of the larger modeling projects utilize the NEMO ocean component, and in the regional/shelf modeling community that focuses development on ROMS.

Numerical methods utilized for many of the community ocean codes have greatly improved during the past decade through intense development and a growing suite of applications. We are thus motivated to offer the following hypothesis.

> PHYSICAL PARAMETERIZATIONS, MORE SO THAN VERTICAL COORDINATE, DETERMINE THE PHYSICAL INTEGRITY OF A GLOBAL OCEAN CLIMATE SIMULATION.

Model/institute	Web site
FESOM/AWI	http://www.awi.de/en
ICOM/Imperial	http://amcg.ese.ic.ac.uk/index.php?title=ICOM
ICON/MPI	http://www.mpimet.mpg.de/en/science/models/icon.html
MPAS-ocean/LANL	public.lanl.gov/ringler/ringler.html
SLIM/Louvain	http://sites-final.uclouvain.be/slim/

Table 5.1.2: A non-exhaustive list of ongoing development efforts utilizing the flexibility of unstructured horizontal meshes. These efforts remain immature for large-scale climate applications, though there are some showing promise (e.g., Timmermann et al., 2009; Ringler et al., 2013). Furthermore, many efforts are not yet supporting open source public use due to their immaturity. Acronyms are the following: FESOM = Finite Element Sea-ice Ocean circulation Model, AWI = Alfred Wegener Institute for Polar and Marine Research in Germany, MPI = Max Planck Institute für Meteorologie in Germany, ICOM = Imperial College Ocean Model in the UK, MPAS = Model for Prediction Across Scales, LANL = Los Alamos National Laboratory in the USA, SLIM = Second-generation Louvain-la-Neuve Ice-ocean Model, Louvain = Louvain-la-Neuve in Belgium.

This hypothesis was untenable at the end of the WOCE era, which was the reason that Griffies et al. (2000a) emphasised vertical coordinates as the central defining feature of a model simulation. However, during the past decade, great strides in numerical methods have removed many of the "features" that distinguish large-scale simulations with different vertical coordinates. Hence, so long as the model configuration resolves flow features admitted by the simulation, there are fewer compelling reasons today than in the year 2000 to choose one vertical coordinate over another.

5.1.2.8. Unstructured horizontal grid meshes

Within the past decade, there has been a growing focus on unstructured horizontal meshes, based on finite volume or finite element methods. These approaches are very distinct from the structured Arakawa grids (Arakawa (1966), Arakawa & Lamb (1981)) used since the 1960s in both the atmosphere and ocean. The main motivation for generalization is to economically capture multiple scales seen in the ocean geometry (i.e., land-sea boundaries) and various scales of oceanic flow (i.e., boundary currents; coastal and shelf processes; active mesoscale eddy regimes). Griffies et al. (2010), Danilov (2013), and Ringler et al. (2013) review recent efforts with applications to the large-scale circulation.

There are many challenges facing finite element and unstructured finite volume methods. Even if the many technical issues listed in Section 4 of Griffies et al. (2010) are overcome, it remains unclear if these approaches will be computationally competitive with structured meshes. That is, more generality in grid meshing comes with a cost in added computational requirements. Nonetheless, the methods are sufficiently compelling to have motivated a new wave in efforts and to have entrained many smart minds towards seeing the ideas fully tested. Table 5.1.2 lists nascent efforts focused on aspects of this approach, with applications in the ocean. We anticipate that within 5-10 years, realistic coupled climate model simulations using unstructured ocean meshes will be realized.

5.1.3. Ocean modeling: science emerging from simulations

We now move from the reductionist theme focused on formulating a physically sound and numerically robust ocean model tool, to the needs of those aiming to use this tool for exploring wholistic questions of ocean circulation and climate. The basis for this exercise in *ocean modeling* is that the model tool has been formulated with sufficient respect to the fundamental physics so that simulated patterns and responses are physically meaningful. A successful ocean modeling activity thus requires a high fidelity numerical tool, a carefully designed experiment, and a variety of analysis methods helping to unravel a mechanistic storyline.

We present a selection of topics relevant to the formulation of a numerical experiment aimed at understanding aspects of the global ocean circulation. Foremost is the issue of how to force an ocean or ocean-ice model. We rely for this discussion on the more thorough treatment given of global ocean-ice modeling in Griffies et al. (2009). In particular, we do not address the extremely difficult and ambiguous issues of model initialization and spinup, leaving such matters to the Griffies et al. (2009) paper for ocean-ice models and Chapter 5.4 of this volume for coupled climate models. Other important issues, such as boundary conditions for regional models and community model experiment strategies, are introduced very briefly. Additionally, we do not consider here the issues of fully coupled climate models (see Chapters 5.4, 5.5, and 5.6).

5.1.3.1. Design considerations for ocean-ice simulations

The ocean is a forced and dissipative system. Forcing occurs at the upper boundary from interactions with the atmosphere, rivers, sea ice, and land ice shelves, and at its lower boundary from the solid earth (see Figure 5.1.1). Forcing also occurs from astronomical effects of the sun and moon to produce tidal motions.[1] Important atmospheric forcing occurs over basin scales, with time scales set by the diurnal cycle, synoptic weather variability (days), the seasonal cycle, and inter-annual fluctuations such as the North Atlantic Oscillation and even longer time scales. Atmospheric momentum and buoyancy fluxes are predominantly responsible for driving the ocean's large scale horizontal and overturning circulations (e.g., Kuhlbrodt et al., 2007). Additional influences include forcing at continental boundaries from river inflow and calving glaciers, as well as in polar regions where sea ice dynamics greatly affect the surface buoyancy fluxes.

Since the successes at reproducing the El Niño-Southern Oscillation phenomenon with linear ocean models in the early 1980s (Philander, 1990), a large number of forced ocean models have demonstrated skill in reproducing the main modes of tropical variability without assimilation of in-situ ocean data, in part because of the linear character of the tropical ocean response to the winds (e.g., Illig et al. (2004)). Furthermore, studies from the past decade show that forced ocean models can, to some extent, reproduce interannual ocean variability in mid-latitudes (e.g., regional patterns of decadal

[1]Climate modelers tend to ignore tidal forcing, but we may soon reach the limitations of assuming tidal motions merely add linearly to the low frequency solution (Schiller & Fiedler, 2007; Arbic et al., 2010).

sea level trends, Lombard et al. (2009)). Hence, a critical issue for the fidelity of an ocean and/or coupled ocean-ice simulation is the forcing methodology.

In the following, we introduce issues associated with how ocean models are forced through boundary fluxes. There is a spectrum of methods that go from the fully coupled climate models detailed in Chapter 5.4, to highly simplified boundary conditions such as damping of surface tracers to an "observed" dataset. Our focus is with ocean and ocean-ice models that are not coupled to an interactive atmosphere. Use of uncoupled ocean models allows one to remove biases inherent in the coupled climate models associated with the prognostic atmosphere component. Yet there is a price to pay when removing feedbacks. We outline these issues in the following.

Air-sea flux formulation for coupled ocean-ice simulations

Ice-ocean fluxes are not observed, and as a result ocean-ice coupled models are more commonly used than ocean-only models for investigations of the basin to global scale forced ocean circulation. Coupled ocean-ice models require surface momentum, heat, and hydrological fluxes to drive the simulated ocean and ice fields. When decoupling the ocean and sea ice models from the atmosphere and land, one must introduce a method to generate these fluxes. One approach is to damp sea surface temperature (SST) and salinity (SSS) to prescribed values. This approach for SST is sensible because SST anomalies experience a local negative feedback (Haney, 1971), whereby they are damped by interactions with the atmosphere. Yet the same is not true for salinity. Furthermore, the associated buoyancy fluxes generated by SST and SSS restoring can be unrealistic (Large et al. (1997), Killworth et al. (2000)). Barnier et al. (1995) introduced another method by combining prescribed fluxes and restoring. However, fluxes from observations and/or reanalysis products have large uncertainties (Taylor (2000), Large & Yeager (2004), Large & Yeager (2009), and Chapter 3.1 in this volume), which can lead to unacceptable model drift (Rosati & Miyakoda, 1988).

Another forcing method prognostically computes turbulent fluxes for heat, moisture, and momentum from a planetary boundary layer scheme (Parkinson & Washington (1979), Barnier (1998)), in addition to applying radiative heating, precipitation and river runoff. Turbulent fluxes are computed from bulk formulae as a function of the ocean surface state (SST and surface currents) and a prescribed atmospheric state (air temperature, humidity, sea level pressure, and wind velocity or wind speed). It is this approach that has been recommended by the CLIVAR Working Group for Ocean Model Development (WGOMD) for running *Coordinated Ocean-ice Reference Experiments* (COREs) (Griffies et al., 2009). Although motivated from its connection to fully coupled climate models, a fundamental limitation of this method relates to the use of a prescribed and nonresponsive atmospheric state that effectively has an infinite heat capacity, moisture capacity, and inertia.

The first attempts to define a forcing protocol for COREs have shown that a restoring to observed sea surface salinity is necessary to prevent multi-decadal drift in the ocean-ice simulations, even though such restoring has no physical basis (see Chapter 6.2 as well as Rivin & Tziperman (1997)). It is thus desirable to use a weak restoring that does not prevent variability in the surface salinity and deep circulation. Unfortunately, when the restoring timescale for SSS is much longer than the effective SST restoring timescale, the thermohaline fluxes move into a regime commonly known as *mixed boundary conditions* (Bryan, 1987), with rather unphysical sensitivities to buoyancy fluxes present in such regimes (Griffies et al., 2009). Furthermore, Griffies et al. (2009) have demonstrated that model solutions are very dependent on the arbitrary strength of the salinity restoring. Artificial salinity restoring may become unnecessary for short term simulations (a few years maximum), if the fidelity of ocean models and the observations of precipitation and runoff improve. For long term simulations, some way of parameterizing the missing feedback between evaporation and precipitation through atmospheric moisture transport is needed.

Another drawback of using a prescribed atmosphere to force an ocean-ice model is the absence of atmospheric response as the ice edge moves. Windy, cold, and dry air is often found near the sea ice edge in nature. Interaction of this air with the ocean leads to large fluxes of latent and sensible heat which cool the surface ocean, as well as evaporation which increases salinity. This huge buoyancy loss increases surface density, which provides a critical element in the downward branch of the thermohaline circulation (e.g., Marshall & Schott, 1999). When the atmospheric state is prescribed, where the simulated sea ice cover increases relative to the observed, the air-sea fluxes are spuriously shut down in the ocean-ice simulation.

Atmospheric datasets and continental runoff

In order to be widely applicable in global ocean-ice modeling, an atmospheric dataset from which to derive surface boundary fluxes should produce near zero global mean heat and freshwater fluxes when used in combination with observed SSTs. This criteria precludes the direct use of atmospheric reanalysis products (see Chapter 3.1). As discussed in Taylor (2000), a combination of reanalysis and remote sensing products provides a reasonable choice to force global ocean-ice models. Furthermore, it is desirable for many research purposes to provide both a repeating "normal" year forcing (NYF) as well as an interannually varying forcing. The dataset compiled by Large & Yeager (2004, 2009) satisfies these desires.

The Large & Yeager (2004, 2009) atmospheric state has been chosen for COREs. The most recent version of the dataset is available from

`http://data1.gfdl.noaa.gov/nomads/forms/core/COREv2.html`,

and it covers the period 1948 to 2009. It is based on NCEP-NCAR reanalysis temperature, wind and humidity, and satellite observations of radiation and precipitation (a climatology is used when satellite products are not available). Similar datasets have been developed by Röske (2006), and more recently by Brodeau et al. (2010), both of which are based on ECMWF products instead of NCEP. The Brodeau et al. (2010) dataset is used in the framework of the European Drakkar project (Drakkar Group, 2007). The availability of multiple forcing datasets is useful in light of large uncertainties of air-sea fluxes. In addition, short term (i.e., interannual) or regional simulations can take advantage of other forcing data, such as scatterometer wind measurements, which have been shown to improve ocean simulations locally (Jiang et al., 2008).

For the multi-decadal global problem, further efforts are needed to improve the datasets used to force ocean models. For example, in the CORE simulations considered by Griffies et al. (2009), interannual variability of river runoff and continental ice melt are not taken into account. However, recent efforts have incorporated both a seasonal cycle and interannually varying climatology into the river runoff, based on the Dai et al. (2009) analysis. Furthermore, the interpretation of trends in the forcing datasets is a matter of debate. For example, the increase of Southern Ocean winds between the early 1970s and the late 1990s is probably exaggerated in the atmospheric reanalyses due to the lack of Southern Ocean observations before 1979. This wind increase is retained in Large & Yeager (2009) used for COREs, whereas Brodeau et al. (2010) attempt to remove it for the Drakkar Forcing. These different choices lead, inevitably, to different decadal trends in the ocean simulations.

Considering the key role of polar regions and their high sensitivity to climate change, ocean-ice simulations will need improved forcings near the polar continents. One issue is taking into account the discharge of icebergs, which can provide a source of freshwater far from the continent, especially in the Antarctic (Jongma et al. (2009), Martin & Adcroft (2010)). The ice-ocean exchanges that occur due to the ocean circulation underneath the ice shelves is an additional complex process that needs to be taken into account, both for the purpose of modeling water mass properties near ice shelves and for the purpose of modeling the flow and stability of continental ice sheets (Chapter 4.6).

Wind stress, surface waves, and surface mixed layer

Mechanical work done by atmospheric winds provides a source of available potential energy that in turn drives much of the ocean circulation. A successful ocean simulation thus requires an accurate mechanical forcing. This task is far from trivial, not only because of wind uncertainties (reanalysis or scatterometer measurements) but also because of uncertainties in the transfer function between 10 meter wind vector and the air-sea wind stress. During the WOCE years, the wind stress was generally prescribed to force ocean models. However, with the generalization of the bulk approach led by Large & Yeager (2004, 2009), modelers started to use a bulk formula to compute the wind stress, with some choosing to do so as a function of the difference between the 10 m wind speed and the ocean velocity (Pacanowski, 1987). The use of such *relative winds* in the stress calculation has a significant damping effect on the surface eddy kinetic energy, up to 50% in the tropical Atlantic and about 10% in mid-latitudes (Eden & Dietze, 2009; Xu & Scott, 2008). Relative winds are clearly what the real system uses to exchange momentum between the ocean and atmosphere, so it is sensible to use such for coupled climate models where the atmosphere responds to the exchange of momentum with the ocean. However, we question the physical relevance of relative winds for the computation of stress in ocean-ice models, where the atmosphere is prescribed.

In general, the classical bulk formulae used to compute the wind stress are being questioned, given the complex processes relating surface wind, surface waves, ocean currents, and high frequency coupling with fine resolution atmosphere and ocean simulations (McWilliams & Sullivan, 2001; Sullivan et al., 2007; Sullivan & McWilliams, 2010). It is potentially important to take into account surface waves and swell not only in the wind stress formulation but also in the parameterization of vertical mixing in the surface boundary layer (Belcher et al., 2012).

Boundary conditions for regional domains

In order to set up a numerical experiment in a regional domain, one needs to represent the lateral exchanges with the rest of the global ocean, at the "open" boundaries of the region of interest. When knowledge of the solution outside the simulated region is limited, an approach similar to the one advocated for ROMS is often used (Marchesiello et al., 2001). This method combines relaxation to a prescribed solution outside the domain with a radiation condition aimed at avoiding spurious reflection or trapping of perturbations at the open boundary. Treguier et al. (2001) have noted that in a realistic primitive equation model where Rossby waves, internal waves and turbulent eddies are present, the phase velocities calculated from the radiation condition have no relationship with the physical processes occurring at the boundary. Despite this fact, radiation appears to have a positive effect on the model solution, perhaps because it introduces stochastic noise in an otherwise over-determined problem. When the solution outside the domain is considered reliable, a "sponge" layer with relaxation to the outside solution is often preferred. Blayo & Debreu (2005) and Herzfeld et al. (2011) provide a review of various methods.

For the purpose of achieving regional simulations of good fidelity, the main progress accomplished in the past decade has come less from improved theory or numerics, and more from the availability of improved global model output that can be used to constrain the boundaries of regional models. These global datasets include operational products, ocean state estimates (Chapters 5.2 and 5.3) and prognostic global simulations (Barnier et al. (2006), Maltrud & McClean (2005)).

The quality of a regional model depends critically on the consistency between the solution outside and inside the domain. Consistency can be ensured by using the same numerical code for the global and regional solution; by using the same (or similar) atmospheric forcing; or by using strategies of grid refinement and nesting. Nesting can be one-way or two-way. For two-way, the large scale or global model is modified at each time step to fit the regional fine-scale solution. Although complex, two-way grid nesting is a promising strategy (Debreu & Blayo, 2008), with impressive applications documenting the role of Agulhas eddies in the variability of the Atlantic meridional overturning (Biastoch et al., 2008). Further considerations are being given to nesting a number of fine resolution regions within a global model.

Community model experiments

In Chapter 7.2 of the first edition of this book, Willebrand and Haidvogel wrote:

> One therefore can argue that the principal limitation for model development arises from the limited manpower in the field, and that having an overly large model diversity may not be the most efficient use of human resources. A more efficient way is the construction of *community models* that can be used by many different groups.

This statement seems prescient in regards to model codes, as noted by the reduced number of codes listed in Table 5.1.1 relative to the Griffies et al. (2000a) review. Additionally, it applies to the coordination of large simulation efforts. Indeed, WOCE has motivated the first Community Model Experiment (CME). This pioneering eddy permitting simulation of the Atlantic circulation (Bryan et al., 1995) and its companion sensitivity experiments have engaged a wide community of oceanographers. The results gave insights into the origin of mesoscale eddies (Beckmann & Haidvogel, 1994), the mechanical energy balance (Treguier, 1992), and mechanisms driving the Atlantic meridional overturning circulation (Redler & Böning, 1997).

As ocean model simulations refine their grid spacing over longer time periods, such community strategies become more useful, whereby simulations are performed in a coordinated fashion by a small group of scientists and distributed to a wider user community. An example of such strategy is carried out within the European DYNAMO project using regional models (Willebrand et al., 1997), and the more recent Drakkar project (Drakkar Group, 2007) that focuses on global ocean-ice models. Global hindcast simulations of the past 50 years have been performed using the NEMO modeling framework for Drakkar (see Table 5.1.1), at different spatial resolutions from 2° to 1/12°, with different forcings and model parameters. A few examples illustrate the usefulness of this approach.

- Analyses of a hierarchy of global simulations with differing resolutions have revealed the role of mesocale eddies in generating large scale, low frequency variability of sea surface height (SSH) (Penduff et al., 2010). Figure 5.1.4 shows that a significant part of the SSH variability observed at periods longer than 18 months is not captured by the coarse resolution version of the model, but is reproduced in an eddy-permitting version, especially in western boundary currents and in the Southern Ocean.

- Using experiments with different strategies for salinity restoring helped assess the robustness of modeled freshwater transports from the Arctic to the Atlantic (Lique et al., 2009).

- A long experiment (obtained by cycling twice over the 50 years of forcing) with a 1/4° global model has been used to estimate the respective role of ocean heat transport and surface heat fluxes in variability of the Atlantic ocean heat content (Grist et al., 2010). The same simulation helped sort out the influence of model drift on the simulated response of the Antarctic Circumpolar Current to the recent increase in Southern ocean winds (Treguier et al., 2010).

5.1.3.2. Analysis of simulations

As models grow more realistic, they become tools of discovery. Important features of the ocean circulation have been discovered in models before being observed in nature. We highlight here two such discoveries.

- Zapiola anticyclone: The Zapiola anticyclone is a large barotropic circulation (~100 Sv) in the Argentine basin south of the Brazil-Malvinas confluence zone. It is a prominent feature in satellite maps of sea surface height variability (Figure 5.1.5), causing a minimum of eddy activity located near 45°S, 45°W inside a characteristic “C”-shaped maximum. The satellite record is now long enough to allow a detailed analysis of its variability (Volkov & Fu, 2008). This region is thus a key location for the evaluation of eddy processes represented in ocean circulation models.

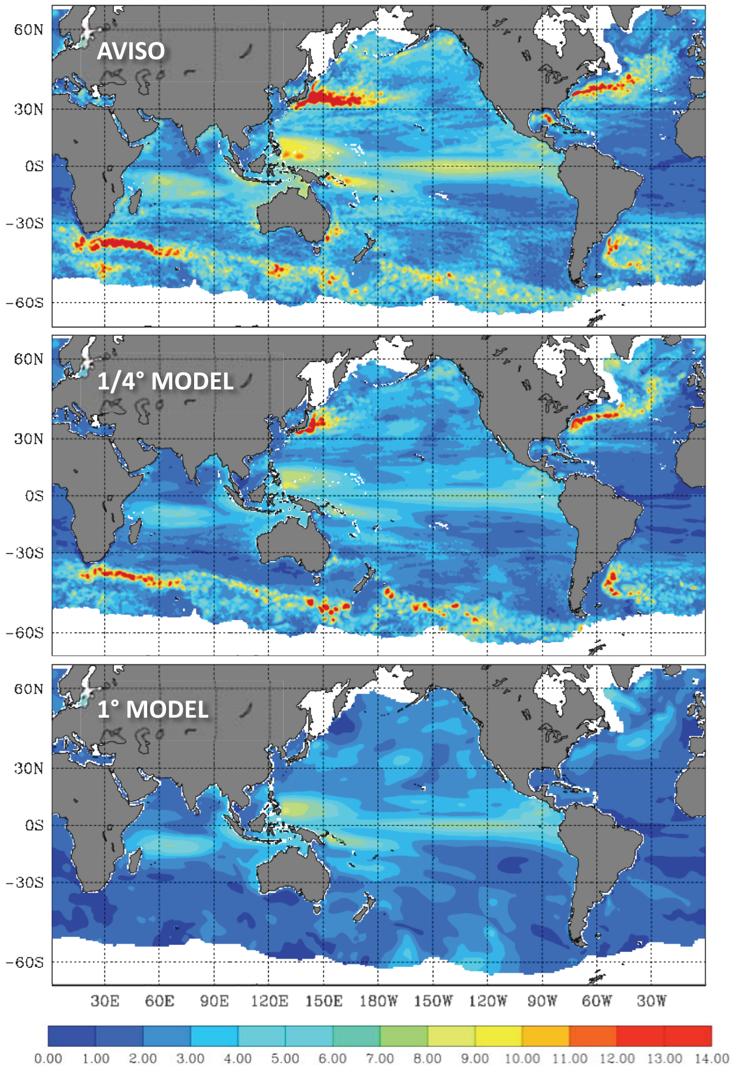

Figure 5.1.4: Variability of the sea surface height for periods longer than 18 months. Top: AVISO altimetric observations (Archiving, Validation, and Interpolation of Satellite Oceanographic; Le Traon et al. (1998); Ducet et al. (2000)); bottom panels: Drakkar model simulations at 1/4° and 1° horizontal grid spacing. Note the absence of much variability in the 1° simulation. Note the enhanced intrinsic ocean variability in the 1/4° model, in contrast to the one-degree model. See Penduff et al. (2010) for details of the models and the temporal filtering.

The Zapiola anticyclone initially appeared in a terrain-following ocean model of the South Atlantic (B. Barnier, personal communication). Yet the circulation was considered a model artefact until observations confirmed its existence (Saunders & King, 1995). As facilitated through studies with ocean models, the Zapiola anticyclone arises from eddy-topography interactions (De Miranda et al., 1999). More precisely, it results from a balance between eddy vorticity fluxes and dissipation, mainly due to bottom drag. For this reason, different models or different numerical choices lead to different simulated strengths of this circulation (Figure 5.1.5).

The Zapiola Drift rises 1100 m above the bottom of the Argentine Abyssal plain. In model simulations that truncate the bottom to be no deeper than 5500 m, the topographic seamount rises only 500 m above the maximum model depth, whereas models with a maximum depth of 6000 m render a far more realistic representation. Merryfield & Scott (2007) argue that the strength of the simulated anticyclone can be dependent on the maximum depth in the model, with shallower representations reducing the strength of the anticyclone.

- Zonal jets in Southwest Pacific: Another model-driven discovery is the existence of zonal jets in the Southwest Pacific, between 30°S and 10°S in the region northeast of Australia. These jets, constrained by topography of the islands, were first documented by the OCCAM eddy permitting model (Webb, 2000). Their existence in the real ocean was later confirmed by satellite altimetry (Hughes, 2002).

Whereas the science of ocean model development consists of the construction of a comprehensive tool, the analysis of ocean simulations mechanistically deconstructs and simplifies the output of the simulation to aid interpretation and to make connections to observations and theory. Analysis methods are prompted by the aims of the research. For example, one may aim to develop a reduced or simplified description, with dominant pieces of the physics identified to aid understanding and provoke further hypotheses, predictions, and theories. By doing so, understanding may arise concerning how the phenomena emerges from the underlying physical laws, making simplifications where appropriate to remove less critical details and to isolate essential mechanisms. The following material represents a non-exhaustive selection of physically-based analysis methods used in ocean modeling. It is notable that options for analyses are enriched, and correspondingly more complex and computationally burdensome, as the model resolution is refined to expand the admitted space and time scales, especially when turbulent elements of the ocean mesoscale and finer scales are included.

Our focus in the following concerns methods used to unravel elements of a particular simulation. To complement these methods, modelers often make use of perturbation approaches whereby elements of the simulation are altered relative to a control case. We have in mind those simulations that alter the boundary fluxes (e.g., remove buoyancy and/or mechanical forcing, swap one forcing dataset for another, modify fluxes over selected geographical regions); alter elements of the model's prognostic equations (e.g., modify subgrid scale parameterizations, remove nonlinear terms in the momentum equation); and refine the horizontal and/or vertical grid spacing. When combined with analysis methods such as those discussed below, these experimental approaches are fundamental to why numerical models are useful for understanding the ocean.

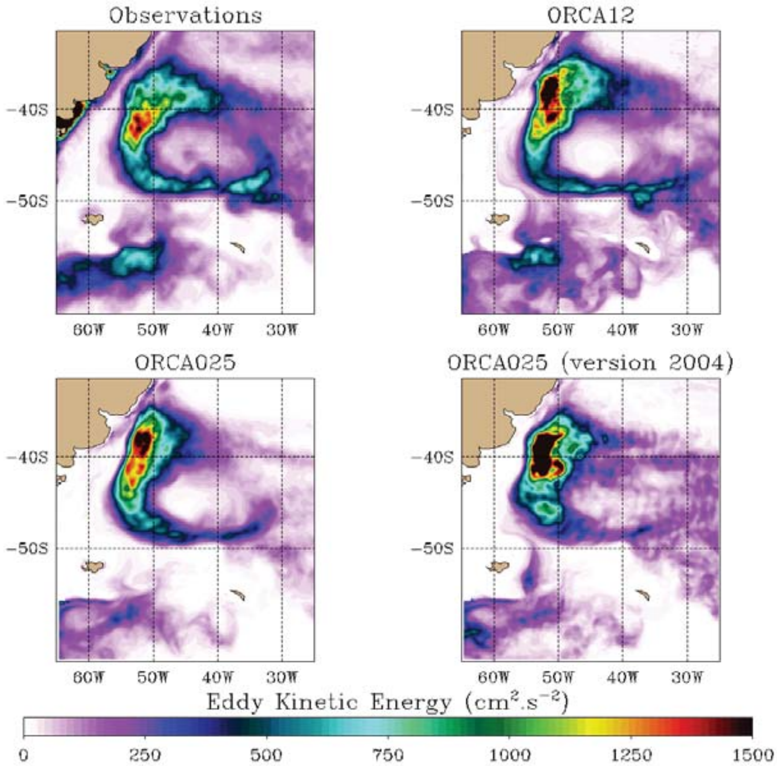

Figure 5.1.5: Variability of surface eddy kinetic energy (EKE) (units of cm^2 s^{-2}) in the Argentine basin of the South Atlantic. (A): EKE of geostrophic currents calculated from altimetric observations (AVISO; Le Traon et al. (1998); Ducet et al. (2000)), based on 10-years mean (October 1992 until February 2002), (B) Drakkar ORCA12 1/12° global model, with simulated data taken from a 10-year mean (1998-2007: last 10 years of a multi-decade run), (C) recent version of the Drakkar ORCA025 1/4° global model, with simulated data taken from years 2000-2009 from a multi-decadal run, (D) same model as (C), but using an older model version with full step bathymetry and a different momentum advection scheme (referenced as ORCA025 G04 in Barnier et al. (2006)), with simulated data taken from 3-year mean (0008-0010: last 3 years from a climatological 10-year run). Note the good agreement with satellite measurements for both the ORCA12 and more recent ORCA025 simulations.

Budget analysis

Identifying dominant terms in the tracer, momentum, and/or vorticity budgets assists in the quest to develop a reduced description, which in turn isolates what physical processes are essential. The straightforward means for doing so consists of a budget analysis, which generally occurs within the framework of the model equations associated with the finite volume budgets as developed in Section 5.1.2.4.

As one example, the mechanical energy cycle of the ocean has been the subject of interest since a series of papers pointed out the potential role of dianeutral mixing as a key energy source for the overturning circulation (Wunsch & Ferrari, 2004; Kuhlbrodt et al., 2007). This work has motivated model-based studies aimed at understanding the energy cycle of the ocean. For example, Gnanadesikan et al. (2005) demonstrated that the link between mechanical mixing and meridional heat transport is rather weak in a climate model with parameterized ocean mesoscale eddies. No unifying view has emerged, but the approach is promising, and will gain momentum when results can be confirmed in more refined eddying global models.

Other examples include budgets of heat or salt in key regions, such as the surface mixed layer (Vialard & Delecluse, 1998) or the subtropical waters (McWilliams et al., 1996). Griffies & Greatbatch (2012) and Palter et al. (2013) present detailed budget analyses focusing on the role of buoyancy on global and regional sea level. Following the pioneering studies of the 1990s, a large number of model-based analyses have considered such tracer budgets in various parts of the ocean. The Argo observing network now makes possible similar analyses that can be partially compared with model results (e.g., de Boisseson et al. (2010)). The confrontation of model-based and observation-based tracer budgets will undoubtedly help improve the representation of mixing processes in models.

Isopycnal watermass analysis

How much seawater or tracer transport passes through an isopycnal layer is a common question asked of model analysts. Relatedly, isopycnal mass analysis as per methods of Walin (1982) have proven of use for inferring the amount of watermass transformation associated with surface boundary fluxes (e.g., Tziperman (1986), Speer & Tziperman (1992), Williams et al. (1995), Marshall et al. (1999), Large & Nurser (2001), Maze et al. (2009), Downes et al. (2011)). Numerical models allow one to go beyond an analysis based solely on surface fluxes, so that interior transformation processes can be directly deduced. For example, the effect of mesoscale eddies on the subduction from the surface mixed layer into the ocean interior has been quantified in the North Atlantic (Costa et al., 2005). By performing a full three-dimensional analysis in a neutral density framework, Iudicone et al. (2008) discovered the essential importance of light penetration on the formation of tropical water masses.

Lagrangian analysis

The Lagrangian parcel perspective often provides useful complementary information relative to the more commonly used Eulerian (fixed point) perspective. One method of Lagrangian analysis proposed by Blanke et al. (1999), as well as Vries & Döös (2001) and van Sebille et al. (2009), uses mass conservation (or volume conservation in Boussinesq models) to decompose mass transport into a large number of "particles", each carrying a tiny fraction of the transport. By following these particles using a Lagrangian algorithm, one can recover the transport of water masses and diagnose their transformation.

Applications of such Lagrangian analyses are numerous. Examples include the tropical Atlantic study of Blanke et al. (1999); the first quantification of the contribution of the Tasman leakage to the global conveyor belt (Speich et al., 2002); the Lagrangian view of the meridional circulation in the Southern Ocean (Döös et al., 2008; Iudicone et al., 2011); and quantification of how water masses are transferred between different regions (Rodgers et al. (2003), Koch-Larrouy et al. (2008), Melet et al. (2011)). These Lagrangian methods have been applied to models absent mesoscale eddies, or only partially admitting such eddies, where a significant part of the dispersion of water masses is parameterized rather than explicitly resolved. The application to eddying models requires large computer resources, and thus have to date only been applied in regional models (Melet et al., 2011). More classical Lagrangian analysis, following arbitrary parcels without relation to the mass transports, have also been applied to eddying models, with a focus on statistical analyses of dispersion (Veneziani et al., 2005).

Passive tracer methods

Many of the ocean's trace constituents have a neglible impact on ocean density, in which case these tracers are dynamically passive (Chapter 5.7). England & Maier-Reimer (2001) review how chemical tracers, such as CFCs and radioactive isotopes, can be used to help understand both the observed and simulated ocean circulation, largely by providing means of tracking parcel motions as well as diagnosing mixing processes. Purposefully released tracers have provided benchmarks for measurements of mixing across the ocean thermocline and abyss (Ledwell et al., 1993; Ledwell & Watson, 1998; Ledwell et al., 2011). Ocean modelers have used similar tracer methods to assess physical and spurious numerical mixing (Section 5.1.2.6). Tracers can also provide estimates for the time it takes water to move from one region to another, with such timescale or generalized age methods exemplified by the many articles in Deleersnijder et al. (2010).

5.1.4. Summary remarks

The evolution of numerical methods, physical parameterizations, and ocean climate applications has been substantial since the first edition of this book in 2001. Today, we better understand the requirements of, for example, maintaining a realistic tropical thermocline essential for simulations of El Niño fluctuations (Meehl et al., 2001), whereas earlier models routinely suffered from an overly diffuse thermocline. We understand far more about the importance of and sensitivity to various physical parameterizations, such as mixing induced by breaking internal waves (Chapter 3.3) and lateral mixing/stirring from mesoscale and submesoscale eddies (Chapter 3.4). Nonetheless, many of the key questions from the first edition remain with us today, in part because the ocean "zoo" (Figure 5.1.1) is so diverse and difficult to tame.

Questions about resolution of physical processes and/or their parameterization sit at the foundation of nearly all compelling questions of ocean models and modeling. What does it mean to fully resolve a physical process? What sorts of numerical methods and/or vertical coordinates are appropriate? Are the multi-scale methods offered by unstructured meshes an optimal means for representing and parameterizing (using scale aware schemes) the multi-scales of ocean fluid dynamics and fractal structure of the land-sea geometry? How well does a parameterization support high fidelity simulations? How do we parameterize a process that is partially resolved without suppressing and/or double-counting those elements of the process that are resolved? Relatedly, how do subgrid scale parameterizations impact on an *effective* resolution? What are the climate impacts from a particular physical process? Are these impacts robust to whether the process is unresolved and parameterized, partially resolved and partially parameterized, or fully resolved? We suggested potential avenues in pursuit of answers to these questions, though noted that robust answers will perhaps only be available after global climate models routinely resolve processes to determine their role in a holistic context.

Amongst the most important transitions to have occurred during the past decade is the growing presence of mesoscale eddying global ocean climate simulations. Changes may appear in air-sea fluxes in coupled simulations due to refined representation of frontal-scale features (Bryan et al., 2010); circulation can be modified through eddy-mean flow interactions (Holland & Rhines, 1980); stochastic features are introduced through eddy fluctuations; and currents interact with a refined representation of bathymetry. Relative to their more laminar predecessors, eddying simulations necessitate enhanced fidelity from numerical methods and require a wide suite of analysis methods to unravel mechanisms. There is progress, but more is required before mesoscale eddying simulations achieve the trust and familiarity required to make them a robust scientific tool for numerical oceanography and climate. In particular, we need a deeper understanding of the generation and decay of mesoscale eddies, both to ensure their proper representation in eddying simulations, and to parameterize in coarse models. We also must address the difficulties associated with managing the huge amounts of simulated data generated by global eddying simulations.

No sound understanding exists of what is required from both grid spacing and numerical methods to fully resolve the mesoscale in global models. The work of Smith et al. (2000) suggest that the mesoscale is resolved so long as the grid spacing is finer than the first baroclinic Rossby radius. This is a sensible hypothesis given that the mesoscale eddy scales are proportional to the Rossby radius, and given that much of the mid-latitude ocean energy is contained in the barotropic and first baroclinic modes. However, this criterion was proposed without a rigorous examination of how important higher modes may be; how sensitive this criteria is to specifics of numerical methods and subgrid scale parameterizations; or whether the criteria is supported by a thorough resolution study. We propose that a solid understanding of the mesoscale eddy resolution question will greatly assist in answering many of the questions regarding the role of the ocean in climate.

A related question concerns the relation between the numerical modeling of mesoscale eddies and dianeutral mixing. Namely, is it sensible to consider mesoscale eddying climate simulations using a model that includes unphysically large spurious dianeutral mixing? Are isopycnal models, or their generalizations to ALE (Arbitrary Lagrangian-Eulerian) methods, the optimal means for ensuring spurious numerical mixing is sufficiently small to accurately capture physical mixing processes, even in the presence of realistic stirring from mesoscale eddies? Or will the traditional level model approaches be enhanced sufficiently to make the modeler's choice based on convenience rather than fundamentals? We conjecture that an answer will be clear within a decade.

As evidenced by the increasing "operational" questions being asked by oceanographers, spanning the spectrum from real time ocean forecasting (Chapter 5.3) to interannual to longer term climate projections (Chapters 5.4, 5.5, 5.6, 5.7) as well as reanalysis and state estimation (Chapter 5.2), numerical oceanography is being increasingly asked to address applied questions that have an impact on decisions reaching outside of science. As with the atmospheric sciences, the added responsibility, and the associated increased visibility, arising from applications brings great opportunities for enhancing ocean science. The increased functionality and applications of ocean models must in turn be strongly coupled to a continued focus on the physics and numerics forming their foundation.

Acknowledgements

We thank WCRP/CLIVAR for sponsoring the Working Group for Ocean Model Development, where the authors have participated since 1999. The presentation in this chapter was greatly assisted by comments from John Church, Carolina Dufour, John Gould, Trevor McDougall, Angélique Melet, Maxim Nikurashin, Gerold Siedler, and an anonymous reviewer. Bernard Barnier kindly provided the Drakkar/ORCA simulation results for Figure 5.1.5. Cathy Raphael kindly drafted Figure 5.1.1.

References

Adcroft, A., & Campin, J.-M. (2004). Rescaled height coordinates for accurate representation of free-surface flows in ocean circulation models. *Ocean Modelling*, *7*, 269–284.

Adcroft, A., Hallberg, R., Dunne, J., Samuels, B., Galt, J., Barker, C., & Payton, D. (2010). Simulations of underwater plumes of dissolved oil in the Gulf of Mexico. *Geophysical Research Letters*, *doi:10.1029/2010GL044689*.

Adcroft, A., & Hallberg, R. W. (2006). On methods for solving the oceanic equations of motion in generalized vertical coordinates. *Ocean Modelling*, *11*, 224–233.

Adcroft, A., Hill, C., & Marshall, J. (1997). Representation of topography by shaved cells in a height coordinate ocean model. *Monthly Weather Review*, *125*, 2293–2315.

Adcroft, A., Scott, J. R., & Marotzke, J. (2001). Impact of geothermal heating on the global ocean circulation. *Geophysical Research Letters*, *28*, 1735–1738.

Arakawa, A. (1966). Computational design for long-term numerical integration of the equations of fluid motion: Two-dimensional incompressible flow. Part 1. *Journal of Computational Physics*, *1*, 119–143.

Arakawa, A., & Lamb, V. (1981). A potential enstrophy and energy conserving scheme for the shallow water equations. *Monthly Weather Review*, *109*, 18–36.

Arbic, B., Wallcraft, A., & Metzger, E. (2010). Concurrent simulation of the eddying general circulation and tides in a global ocean model. *Ocean Modelling*, *32*, 175–187.

Barnier, B. (1998). Forcing the ocean. In E. P. Chassignet, & J. Verron (Eds.), *Ocean Modeling and Parameterization* (pp. 45–80). Kluwer volume 516 of *NATO ASI Mathematical and Physical Sciences Series*.

Barnier, B., Madec, G., Penduff, T., Molines, J., Treguier, A., Sommer, J. L., Beckmann, A., Biastoch, A., Böning, C. W., Dengg, J., Derval, C., Durand, E., Gulev, S., Remy, E., Talandier, C., Theetten, S., Maltrud, M., McClean, J., & Cuevas, B. D. (2006). Impact of partial steps and momentum advection schemes in a global ocean circulation model at eddy permitting resolution. *Ocean Dynamics*, *56*, 543–567.

Barnier, B., Siefridt, L., & Marchesiello, P. (1995). Thermal forcing for a global ocean circulation model using a three-year climatology of ECMWF analyses. *Journal of Marine Research*, *6*, 363–380.

Bates, M., Griffies, S. M., & England, M. (2012a). A dynamic, embedded Lagrangian model for ocean climate models, Part I: Theory and implementation. *Ocean Modelling*, .

Bates, M., Griffies, S. M., & England, M. (2012b). A dynamic, embedded Lagrangian model for ocean climate models, Part II: Idealised overflow tests. *Ocean Modelling*, .

Beckmann, A. (1998). The representation of bottom boundary layer processes in numerical ocean circulation models. In E. P. Chassignet, & J. Verron (Eds.), *Ocean Modeling and Parameterization* (pp. 135–154). Kluwer volume 516 of *NATO ASI Mathematical and Physical Sciences Series*.

Beckmann, A., & Döscher, R. (1997). A method for improved representation of dense water spreading over topography in geopotential-coordinate models. *Journal of Physical Oceanography*, *27*, 581–591.

Beckmann, A., & Haidvogel, D. (1993). Numerical simulation of flow around a tall isolated seamount. Part I: Problem formulation and model accuracy. *Journal of Physical Oceanography*, *23*, 1736–1753.

Beckmann, A., & Haidvogel, D. (1994). On the generation and role of eddy variability in the central North Atlantic Ocean. *Journal of Geophysical Research*, *99*, 20381–20391.

Belcher, S., Grant, A., Hanley, K., Fox-Kemper, B., Van Roekel, L., Sullivan, P., Large, W., Brown, A., Hines, A., Calvert, D., Rutgersson, A., Petterson, H., Bidlot, J., Janssen, P., & Polton, J. A. (2012). A global perspective on Langmuir turbulence in the ocean surface boundary layer. *Geophysical Research Letters*, *39-L18605*, doi:10.1029/2012GL052932.

Berlov, P. (2005). Random-forcing model of the mesoscale oceanic eddies. *Journal of Fluid Mechanics*, *529*, 71–95.

Biastoch, A., Böning, C., & Lutjeharms, J. (2008). Agulhas leakage dynamics affects decadal variability in Atlantic overturning circulation. *Nature*, *456:7221*, 489–492.

Blanke, B., Arhan, M., Madec, G., & Roche, S. (1999). Warm water paths in the equatorial Atlantic as diagnosed with a general circulation model. *Journal of Physical Oceanography*, *29*, 2753–2768.

Blayo, E., & Debreu, L. (2005). Revisiting open boundary conditions from the point of view of characteristic variables. *Ocean Model.*, *9*, 231–252.

Bleck, R. (1998). Ocean modeling in isopycnic coordinates. In E. P. Chassignet, & J. Verron (Eds.), *Ocean Modeling and Parameterization* (pp. 423–448). Kluwer volume 516 of *NATO ASI Mathematical and Physical Sciences Series*.

Bleck, R. (2002). An oceanic general circulation model framed in hybrid isopycnic-cartesian coordinates. *Ocean Modelling*, *4*, 55–88.

Boccaletti, G., Ferrari, R., & Fox-Kemper, B. (2007). Mixed layer instabilities and restratification. *Journal of Physical Oceanography*, *35*, 1263–1278.

de Boisseson, E., Thierry, V., Mercier, H., & Caniaux, G. (2010). Mixed layer heat budget in the iceland basin from argo. *Journal of Geophysical Research*, *115*, C10055.

Böning, C. W., Dispert, A., Visbeck, M., Rintoul, S., & Schwarzkopf, F. (2008). The response of the Antarctic Circumpolar Current to recent climate change. *Nature Geoscience*, *1*, 864–869.

Brankart, J.-M. (2013). Impact of uncertainties in the horizontal density gradient upon low resolution global ocean modelling. *Ocean Modelling*, *submitted*.

Brodeau, L., Barnier, B., Treguier, A., Penduff, T., & Gulev, S. (2010). An ERA40-based atmospheric forcing for global ocean circulation models. *Ocean Modelling*, *31*, 88–104.

Bryan, F. (1987). Parameter sensitivity of primitive equation ocean general circulation models. *Journal of Physical Oceanography*, *17*, 970–985.

Bryan, F., Böning, C., & Holland, W. (1995). On the mid-latitude circulation in a high resolution model of the North Atlantic. *Journal of Physical Oceanography*, *25*, 289–305.

Bryan, F., Thomas, R., Dennis, J., Chelton, D., Loeb, N., & McClean, J. (2010). Frontal scale air-sea interaction in high-resolution coupled climate models. *Journal of Climate*, *23*, 6277–6291.

Bryan, K., & Lewis, L. J. (1979). A water mass model of the world ocean. *Journal of Geophysical Research*, *84*, 2503–2517.

Bryan, K., Manabe, S., & Pacanowski, R. C. (1975). A global ocean-atmosphere climate model. Part II. The oceanic circulation. *Journal of Physical Oceanography*, *5*, 30–46.

Campin, J.-M., & Goosse, H. (1999). Parameterization of density-driven downsloping flow for a coarse-resolution ocean model in z-coordinate. *Tellus*, *51A*, 412–430.

Campin, J.-M., Marshall, J., & Ferreira, D. (2011). Super-parameterization in ocean modeling: Application to deep convection. *Ocean Modelling*, *36*, 90–101.

Cavaleri, L., Fox-Kemper, B., & Hemer, M. (2012). Wind waves in the coupled climate system. *Bulletin of the American Meteorological Society*, *93*, 1651–1661.

Chaikin, P. M., & Lubensky, T. C. (1995). *Principles of Condensed Matter Physics*. Cambridge, United Kingdom: Cambridge University Press.

Costa, M. D., Mercier, H., & Treguier, A.-M. (2005). Effects of the mixed layer time variability on kinematic subduction rate diagnostics. *Journal of Physical Oceanography*, *35*, 427–443.

Cox, M. D. (1984). *A Primitive Equation, 3-Dimensional Model of the Ocean*. Princeton, USA: NOAA/Geophysical Fluid Dynamics Laboratory.

Dai, A., Qian, T., Trenberth, K., & Milliman, J. (2009). Changes in continental freshwater discharge from 1948-2004. *Journal of Climate*, *22*, 2773–2791.

Danabasoglu, G., Large, W., & Briegleb, B. (2010). Climate impacts of parameterized nordic sea overflows. *Journal of Geophysical Research*, *115, C11005*, doi:10.1029/2010JC006243.

Danilov, S. D. (2013). Ocean modeling on unstructured meshes. *Ocean Modelling*, *...*, doi.org/10.1016/j.ocemod.2013.05.005.

Davis, R. E. (1994a). Diapycnal mixing in the ocean: equations for large-scale budgets. *Journal of Physical Oceanography*, *24*, 777–800.

Davis, R. E. (1994b). Diapycnal mixing in the ocean: the Osborn-Cox model. *Journal of Physical Oceanography*, *24*, 2560–2576.

De Miranda, A., Barnier, B., & Dewar, W. (1999). On the dynamics of the Zapiola Anticyclone. *Journal of Geophysical Research*, *104*, 21137–21149.

Debreu, L., & Blayo, E. (2008). Two-way embedding algorithms: a review. *Ocean Dynamics*, *58*, 415–428.

DeGroot, S. R., & Mazur, P. (1984). *Non-Equilibrium Thermodynamics*. New York: Dover Publications. 510 pp.

Deleersnijder, E., & Beckers, J.-M. (1992). On the use of the $\sigma-$coordinate system in regions of large bathymetric variations. *Journal of Marine Systems*, *3*, 381–390.

Deleersnijder, E., Cornaton, F., Haine, T., Vanclooster, M., & Waugh, D. W. (2010). Tracer and timescale methods for understanding complex geophysical and environmental fluid flows. *Environmental Fluid Mechanics*, *10*, DOI 10.1007/s10652–009–9164–1.

Delworth, T. L., Rosati, A., Anderson, W., Adcroft, A. J., Balaji, V., Benson, R., Dixon, K., Griffies, S. M., Lee, H.-C., Pacanowski, R. C., Vecchi, G. A., Wittenberg, A. T., Zeng, F., & Zhang, R. (2012). Simulated climate and climate change in the GFDL CM2.5 high-resolution coupled climate model. *Journal of Climate*, *25*, 2755–2781.

Denbo, D., & Skyllingstad, E. (1996). An ocean large-eddy simulation model with application to deep convection in the Greenland Sea. *Journal of Geophysical Research*, *101*, 1095–1110.

DeSzoeke, R. A. (2009). Isentropic averaging. *Journal of Marine Research*, *67*, 533–567.

DeSzoeke, R. A., & Bennett, A. F. (1993). Microstructure fluxes across density surfaces. *Journal of Physical Oceanography*, *23*, 2254–2264.

DeSzoeke, R. A., & Samelson, R. M. (2002). The duality between the Boussinesq and non-Boussinesq hydrostatic equations of motion. *Journal of Physical Oceanography*, *32*, 2194–2203.

Dietrich, D., Marietta, M., & Roache, P. (1987). An ocean modeling system with turbulent boundary layers and topography: Part 1. numerical studies of small island wakes in the ocean. *International Journal of Numerical Methods in Fluids*, *7*, 833–855.

Donea, J., Huerta, A., Ponthot, J.-P., & Rodríguez-Ferran, A. (2004). Arbitrary Lagrangian-Eulerian methods. In E. Stein, R. de Borst, & T. J. R. Hughes (Eds.), *Encyclopedia of Computational Mechanics* chapter 14. John Wiley and Sons.

Döös, K., Nycander, J., & Coward, A. (2008). Lagrangian decomposition of the Deacon Cell. *Journal of Geophysical Research-Oceans*, *113*.

Downes, S. M., Gnanadesikan, A., Griffies, S. M., & Sarmiento, J. (2011). Water mass exchange in the Southern Ocean in coupled climate models. *Journal of Physical Oceanography*, *41*, 1756–1771.

Drakkar Group (2007). Eddy-permitting ocean circulation hindcasts of past decades. *CLIVAR Exchanges*, *42*, 8–10.

Ducet, N., Le Traon, P.-Y., & Reverdin, G. (2000). Global high-resolution mapping of ocean circulation from TOPEX/Poseidon and ERS-1 and -2. *Journal of Geophysical Research*, *105*, 19477–19498.

Dunne, J. P., John, J. G., Hallberg, R. W., Griffies, S. M., Shevliakova, E. N., Stouffer, R. J., Krasting, J. P., Sentman, L. A., Milly, P. C. D., Malyshev, S. L., Adcroft, A. J., Cooke, W., Dunne, K. A., Harrison, M. J., Levy, H., Samuels, B. L., Spelman, M., Winton, M., Wittenberg, A. T., Phillips, P. J., & Zadeh, N. (2012). GFDLs ESM2 global coupled climate-carbon Earth System Models Part I: Physical formulation and baseline simulation characteristics. *Journal of Climate*, *25*, 6646–6665.

Eckart, C. (1948). An analysis of the stirring and mixing processes in incompressible fluids. *Journal of Marine Research*, *7*, 265–275.

Eden, C., & Dietze, H. (2009). Effects of mesoscale eddy/wind interactions on biological new production and eddy kinetic energy. *Journal of Geophysical Research*, *114*, C05023.

Eden, C., Greatbatch, R., & Olbers, D. (2007). Interpreting eddy fluxes. *Journal of Physical Oceanography*, *37*, 1282–1296.

Emile-Geay, J., & Madec, G. (2009). Geothermal heating, diapycnal mixing and the abyssal circulation. *Ocean Science*, *5*, 203–217.

England, M. H., & Maier-Reimer, E. (2001). Using chemical tracers to assess ocean models. *Reviews of Geophysics*, *39*, 29–70.

Farneti, R., Delworth, T., Rosati, A., Griffies, S. M., & Zeng, F. (2010). The role of mesoscale eddies in the rectification of the Southern Ocean response to climate change. *Journal of Physical Oceanography*, *40*, 1539–1557.

Farneti, R., & Gent, P. (2011). The effects of the eddy-induced advection coefficient in a coarse-resolution coupled climate model. *Ocean Modelling*, *39*, 135–145.

Fox-Kemper, B., Ferrari, R., & Hallberg, R. (2008). Parameterization of mixed layer eddies. I: Theory and diagnosis. *Journal of Physical Oceanography*, *38*, 1145–1165.

Fox-Kemper, B., & Menemenlis, D. (2008). Can large eddy simulation techniques improve mesoscale rich ocean models? In M. Hecht, & H. Hasumi (Eds.), *Eddy resolving ocean models* Geophysical Monograph 177 (pp. 319–338). American Geophysical Union.

Frankignoul, C., & Hasselmann, K. (1977). Stochastic climate models. Part II: Application to sea-surface temperature variability and thermocline variability. *Tellus*, *29*, 284–305.

Gent, P., & Danabasoglu, G. (2011). Response of increasing Southern Hemisphere winds in CCSM4. *Journal of Climate*, *24*, 4992–4998.

Gent, P. R., & McWilliams, J. C. (1990). Isopycnal mixing in ocean circulation models. *Journal of Physical Oceanography*, *20*, 150–155.

Gent, P. R., Willebrand, J., McDougall, T. J., & McWilliams, J. C. (1995). Parameterizing eddy-induced tracer transports in ocean circulation models. *Journal of Physical Oceanography*, *25*, 463–474.

Gill, A. (1982). *Atmosphere-Ocean Dynamics* volume 30 of *International Geophysics Series*. London: Academic Press. 662 + xv pp.

Gnanadesikan, A., Slater, R. D., Swathi, P. S., & Vallis, G. K. (2005). The energetics of ocean heat transport. *Journal of Climate*, *17*, 26042616.

Goldberg, D., Little, C., Sergienko, O., Gnanadesikan, A., Hallberg, R., & Oppenheimer, M. (2012). Investigation of land ice-ocean interaction with a fully coupled ice-ocean model: 1. Model description and behavior. *Journal of Geophysical Research*, *117-F02037*, doi:10.1029/2011JF002246.

Grabowski, W. (2001). Coupling cloud processes with the large-scale dynamics using the Cloud-Resolving Convection Parameterization (CRCP). *Journal of Atmospheric Sciences*, *58*, 978–997.

Greatbatch, R. J. (1994). A note on the representation of steric sea level in models that conserve volume rather than mass. *Journal of Geophysical Research*, *99*, 12767–12771.

Greatbatch, R. J., & McDougall, T. J. (2003). The non-Boussinesq temporal-residual-mean. *Journal of Physical Oceanography*, *33*, 1231–1239.

Gregg, M., Sanford, T., & Winkel, D. (2003). Reduced mixing from the breaking of internal waves in equatorial waters. *Nature*, *422*, 513–515.

Griffies, S. M. (1998). The Gent-McWilliams skew-flux. *Journal of Physical Oceanography*, *28*, 831–841.

Griffies, S. M. (2004). *Fundamentals of Ocean Climate Models*. Princeton, USA: Princeton University Press. 518+xxxiv pages.

Griffies, S. M., & Adcroft, A. J. (2008). Formulating the equations for ocean models. In M. Hecht, & H. Hasumi (Eds.), *Eddy resolving ocean models* Geophysical Monograph 177 (pp. 281–317). American Geophysical Union.

Griffies, S. M., Adcroft, A. J., Banks, H., Böoning, C. W., Chassignet, E. P., Danabasoglu, G., Danilov, S., Deleersnijder, E., Drange, H., England, M., Fox-Kemper, B., Gerdes, R., Gnanadesikan, A., Greatbatch, R. J., Hallberg, R., Hanert, E., Harrison, M. J., Legg, S. A., Little, C. M., Madec, G., Marsland, S., Nikurashin, M., Pirani, A., Simmons, H. L., Schröoter, J., Samuels, B. L., Treguier, A.-M., Toggweiler, J. R., Tsujino, H., Vallis, G. K., & White, L. (2010). Problems and prospects in large-scale ocean circulation models. In J. Hall, D. Harrison, & D. Stammer (Eds.), *Proceedings of the OceanObs09 Conference: Sustained Ocean Observations and Information for Society, Venice, Italy, 21-25 September 2009*. ESA Publication WPP-306 volume 2.

Griffies, S. M., Biastoch, A., Böning, C. W., Bryan, F., Danabasoglu, G., Chassignet, E., England, M. H., Gerdes, R., Haak, H., Hallberg, R. W., Hazeleger, W., Jungclaus, J., Large, W. G., Madec, G., Pirani, A., Samuels, B. L., Scheinert, M., Gupta, A. S., Severijns, C. A., Simmons, H. L., Treguier, A. M., Winton, M., Yeager, S., & Yin, J. (2009). Coordinated Ocean-ice Reference Experiments (COREs). *Ocean Modelling*, *26*, 1–46.

Griffies, S. M., Böning, C. W., Bryan, F. O., Chassignet, E. P., Gerdes, R., Hasumi, H., Hirst, A., Treguier, A.-M., & Webb, D. (2000a). Developments in ocean climate modelling. *Ocean Modelling*, *2*, 123–192.

Griffies, S. M., & Greatbatch, R. J. (2012). Physical processes that impact the evolution of global mean sea level in ocean climate models. *Ocean Modelling*, *51*, 37–72.

Griffies, S. M., & Hallberg, R. W. (2000). Biharmonic friction with a Smagorinsky viscosity for use in large-scale eddy-permitting ocean models. *Monthly Weather Review*, *128*, 2935–2946.

Griffies, S. M., Pacanowski, R., Schmidt, M., & Balaji, V. (2001). Tracer conservation with an explicit free surface method for *z*-coordinate ocean models. *Monthly Weather Review*, *129*, 1081–1098.

Griffies, S. M., Pacanowski, R. C., & Hallberg, R. W. (2000b). Spurious diapycnal mixing associated with advection in a *z*-coordinate ocean model. *Monthly Weather Review*, *128*, 538–564.

Griffies, S. M., Winton, M., Donner, L. J., Downes, S. M., Farneti, R., Gnanadesikan, A., Horowitz, L. W., Hurlin, W. J., Lee, H.-C., Liang, Z., Palter, J. B., Samuels, B. L., Wittenberg, A. T., Wyman, B. L., Yin, J., & Zadeh, N. T. (2011). GFDL's CM3 coupled climate model: Characteristics of the ocean and sea ice simulations. *Journal of Climate*, *24*, 3520–3544.

Grinstein, F. F., Margolin, L. G., & Rider, W. J. (2007). A rationale for implicit LES. In F. Grinstein, L. Margolin, & W. Rider (Eds.), *Implicit Large Eddy Simulation: Computing Turbulent Fluid Dynamics*. Cambridge University Press.

Grist, J. P., Josey, S. A., Marsh, R., Good, S. A., Coward, A., de Cuevas, B., Alderson, S., New, A., & Madec, G. (2010). The roles of surface heat flux and ocean heat transport convergence in determining Atlantic Ocean temperature variability. *Ocean Dynamics*, *60*, 771–790.

Hall, A., & Manabe, S. (1997). Can local, linear stochastic theory explain sea surface temperature and salinity variability? *Climate Dynamics*, *13*, 167–180.

Hallberg, R. W. (2003). The suitability of large-scale ocean models for adapting parameterizations of boundary mixing and a description of a refined bulk mixed layer model. In P. Müller, & C. Garrett (Eds.), *Near-Boundary Processes and Their Parameterization* Proceedings of the 13th 'Aha Huliko'a Hawaiian Winter Workshop (pp. 187–203). University of Hawaii at Manoa.

Haney, R. L. (1971). Surface thermal boundary conditions for ocean circulation models. *Journal of Physical Oceanography*, *1*, 241–248.

Haney, R. L. (1991). On the pressure gradient force over steep topography in sigma-coordinate ocean models. *Journal of Physical Oceanography*, *21*, 610–619.

Hasselmann, K. (1976). Stochastic climate models. Part I: Theory. *Tellus*, *28*, 473–485.

Herzfeld, M., Schmidt, M., Griffies, S. M., & Liang, Z. (2011). Realistic test cases for limited area ocean modelling. *Ocean Modelling*, *37*, 1–34.

Hesselberg, T. (1926). Die Gesetze der ausgeglichenen atmosphaerischen Bewegungen. *Beiträgeder Physik der freien Atmosphere*, *12*, 141–160.

Hill, C., Ferreira, D., Campin, J.-M., Marshall, J., Abernathey, R., & Barrier, N. (2012). Controlling spurious diapyncal mixing in eddy-resolving height-coordinate ocean models–insights from virtual deliberate tracer release experiments. *Ocean Modelling*, *45–46*, 14–26.

Hofmann, M., & Morales-Maqueda, M. (2011). The response of Southern Ocean eddies to increased midlatitude westerlies: A non-eddy resolving model study. *Geophysical Research Letters*, *38 (L03605)*, doi:10.1029/2010GL045972.

Holland, W. R., & Rhines, P. B. (1980). An example of eddy-induced ocean circulation. *Journal of Physical Oceanography*, *10*, 1010–1031.

Holloway, G. (1986). Eddies, waves, circulation, and mixing: statistical geofluid mechanics. *Annual Review of Fluid Mechanics*, *18*, 91–147.

Holloway, G. (1989). Subgridscale representation. In D. L. Anderson, & J. Willebrand (Eds.), *Oceanic Circulation Models: Combining Data and Dynamics* (pp. 513–593). Kluwer Academic Publishers volume 284 of *NATO ASI Series. Series C*.

Holloway, G. (1992). Representing topographic stress for large-scale ocean models. *Journal of Physical Oceanography*, *22*, 1033–1046.

Huang, R. X., Jin, X., & Zhang, X. (2001). An oceanic general circulation model in pressure coordinates. *Advances in Atmospheric Physics*, *18*, 1–22.

Hughes, C. (2002). Zonal jets in and near the Coral Sea seen by satellite altimetry. *Geophysical Research Letters*, *29*, 1330.

Ilicak, M., Adcroft, A. J., Griffies, S. M., & Hallberg, R. W. (2012). Spurious dianeutral mixing and the role of momentum dissipation. *Ocean Modelling*, *45–46*, 37–58.

Illig, S., Dewitte, B., Ayoub, N., du Penhoat, Y., abd P. De Mey, G. R., Bonjean, F., & Lagerloef, G. S. E. (2004). Interannual long equatorial waves in the tropical Atlantic from a high-resolution ocean general circulation model experiment in 1981–2000. *Journal of Geophysical Research*, *109-C02022*, doi:10.1029/2003JC001771.

IOC, SCOR, & IAPSO (2010). *The international thermodynamic equation of seawater-2010: calculation and use of thermodynamic properties*. available from http://www.TEOS-10.org: Intergovernmental Oceanographic Commission, Manuals and Guides No. 56, UNESCO. 196pp.

Iudicone, D., Madec, G., & McDougall, T. J. (2008). Water-mass transformations in a neutral density framework and the key role of light penetration. *Journal of Physical Oceanography*, *38*, 1357–1376.

Iudicone, D., Rodgers, K., Stendardo, I., Aumont, O., Madec, G., Bopp, L., Mangoin, O., & d'Alcala, M. R. (2011). Water masses as a unifying framework for understanding the Southern Oocean Carbon Cycle. *Biogeosciences*, *8*, 1031–1052.

Jackson, L., Hallberg, R., & Legg, S. (2008). A parameterization of shear-driven turbulence for ocean climate models. *Journal of Physical Oceanography*, *38*, 1033–1053.

Jiang, C., Thompson, L., & Kelly, K. (2008). Equatorial influence of QuikSCAT winds in an isopycnal ocean model compared to NCEP2 winds. *Ocean Modelling*, *24*, 65–71.

Jochum, M., , Danabasoglu, G., Holland, M., Kwon, Y.-O., & Large, W. (2008). Ocean viscosity and climate. *Journal of Geophysical Research*, *114 C06017*, doi:10.1029/2007JC004515.

Jochum, M. (2009). Impact of latitudinal variations in vertical diffusivity on climate simulations. *Journal of Geophysical Research*, *114 C01010*, doi:10.1029/2008JC005030.

Jones, H., & Marshall, J. (1993). Convection with rotation in a neutral ocean: a study of open-ocean deep convection. *Journal of Physical Oceanography*, *23*, 1009–1039.

Jongma, J., Driesschaert, E., Fichefet, T., Goosse, H., & Renssen, H. (2009). The effect of dynamic-thermodynamic icebergs on the Southern Ocean climate in a three-dimensional model. *Ocean Modelling*, *26*, 104–113.

Khairoutdinov, M., DeMott, C., & Randall, D. (2008). Evaluation of the simulated interannual and subseasonal variability in an AMIP-style simulation using the CSU Multiscale Modeling Framework. *Journal of Climate*, *21*, 413–431.

Killworth, P. D., & Edwards, N. (1999). A turbulent bottom boundary layer code for use in numerical ocean models. *Journal of Physical Oceanography*, *29*, 1221–1238.

Killworth, P. D., Smeed, D., & Nurser, A. (2000). The effects on ocean models of relaxation toward observations at the surface. *Journal of Physical Oceanography*, *30*, 160–174.

Kitsios, V., Frederiksen, J. S., & Zidikheri, M. J. (2013). Scaling laws for parameterisations of subgrid eddy-eddy interactions in simulations of oceanic circulations. *Ocean Modelling*, *...*, doi.org/10.1016/j.ocemod.2013.05.001.

Klein, P., & Lapeyre, G. (2009). The oceanic vertical pump induced by mesoscale and submesoscale turbulence. *Annual Reviews of Marine Science*, *1*, 351–375.

Klinger, B. A., Marshall, J., & Send, U. (1996). Representation of convective plumes by vertical adjustment. *Journal of Geophysical Research*, *101*, 18175–18182.

Klocker, A., & McDougall, T. J. (2010). Influence of the nonlinear equation of state on global estimates of dianeutral advection and diffusion. *Journal of Physical Oceanography*, *40*, 1690–1709.

Koch-Larrouy, A., Madec, G., Blanke, B., & Molcard, R. (2008). Water mass transformation along the Indonesian throughflow in an OGCM. *Journal of Physical Oceanography*, *58*, 289–309.

Kopp, R. E., Mitrovica, J. X., Griffies, S. M., Yin, J., Hay, C. C., & Stouffer, R. J. (2010). The impact of Greenland melt on regional sea level: a preliminary comparison of dynamic and static equilibrium effects. *Climatic Change Letters*, *103*, 619–625.

Kuhlbrodt, T., Griesel, A., Montoya, M., Levermann, A., Hofmann, M., & Rahmstorf, S. (2007). On the driving processes of the Atlantic meridional overturning circulation. *Reviews of Geophysics*, *45*, doi:10.1029/2004RG000166.

Kunze, E., Firing, E., Hummon, J. M., Chereskin, T. K., & Thurnherr, A. M. (2006). Global Abyssal Mixing Inferred from Lowered ADCP Shear and CTD Strain Profiles. *Journal of Physical Oceanography*, *36*, 1553–1576.

Kunze, E., & Sanford, T. B. (1996). Abyssal mixing: where it is not. *Journal of Physical Oceanography*, *26*, 2286–2296.

Laanaia, N., Wirth, A., Molines, J., Barnier, B., & Verron, J. (2010). On the numerical resolution of the bottom layer in simulations of oceanic gravity currents. *Ocean Science*, *6*, 563–572.

Large, W., McWilliams, J., & Doney, S. (1994). Oceanic vertical mixing: a review and a model with a nonlocal boundary layer parameterization. *Reviews of Geophysics*, *32*, 363–403.

Large, W., & Yeager, S. (2004). Diurnal to decadal global forcing for ocean and sea-ice models: the data sets and flux climatologies. NCAR Technical Note: NCAR/TN-460+STR. CGD Division of the National Center for Atmospheric Research.

Large, W. B., & Nurser, A. G. (2001). Ocean surface water mass transformation. In G. Seidler, J. Church, & J. Gould (Eds.), *Ocean Circulation and Climate* (pp. 317–336). San Diego: Academic Press volume 77 of *International Geophysics Series*.

Large, W. G., Danabasoglu, G., Doney, S. C., & McWilliams, J. C. (1997). Sensitivity to surface forcing and boundary layer mixing in a global ocean model: annual-mean climatology. *Journal of Physical Oceanography*, *27*, 2418–2447.

Large, W. G., Danabasoglu, G., McWilliams, J. C., Gent, P. R., & Bryan, F. O. (2001). Equatorial circulation of a global ocean climate model with anisotropic horizontal viscosity. *Journal of Physical Oceanography*, *31*, 518–536.

Large, W. G., & Yeager, S. (2009). The global climatology of an interannually varying air-sea flux data set. *Climate Dynamics*, *33*, 341–364.

Le Sommer, J., Penduff, T., Theetten, S., Madec, G., & Barnier, B. (2009). How momentum advection schemes influence current-topography interactions at eddy permitting resolution. *Ocean Modelling*, *29*, 1–14.

Le Traon, P.-Y., Nadal, F., & Ducet, N. (1998). An improved mapping metod of multi-satellite altimeter data. *Journal of Atmospheric and Oceanic Technology*, *15*, 522–534.

Leclair, M., & Madec, G. (2011). $\tilde{z}$-coordinate, an arbitrary LagrangianEulerian coordinate separating high and low frequency motions. *Ocean Modelling*, *37*, 139–152.

Ledwell, J. R., St.Laurent, L., Girton, J., & Toole, J. (2011). Diapycnal mixing in the Antarctic Circumpolar Current. *Journal of Physical Oceanography*, *41*, 241–246.

Ledwell, J. R., & Watson, A. J. (1998). Mixing of a tracer in the pycnocline. *Journal of Geophysical Research*, *103*, 21499–21529.

Ledwell, J. R., Watson, A. J., & Law, C. S. (1993). Evidence for slow mixing across the pycnocline from an open-ocean tracer-release experiment. *Nature*, *364*, 701–703.

Legg, S. (2012). Overflows and convectively driven flows. In E. Chassignet, C. Cenedese, & J. Verron (Eds.), *Buoyancy-Driven flows*. Cambridge UK: Cambridge University Press.

Legg, S., Briegleb, B., Chang, Y., Chassignet, E. P., Danabasoglu, G., Ezer, T., Gordon, A. L., Gries, S. M., Hallberg, R. W., Jackson, L., Large, W., Özgökmen, T. M., Peters, H., Price, J., Riemenschneider, U., Wu, W., Xu, X., & Yang, J. (2009). Improving oceanic overow representation in climate models: The Gravity Current Entrainment Climate Process Team. *Bulletin of the American Meteorological Society*, *90*, 657–670.

Legg, S., Hallberg, R., & Girton, J. (2006). Comparison of entrainment in overflows simulated by z-coordinate, isopycnal and non-hydrostatic models. *Ocean Modelling*, *11*, 69–97.

Legg, S., Jackson, L., & Hallberg, R. (2008). Eddy-resolving modeling of overflows. In M. Hecht, & H. Hasumi (Eds.), *Eddy resolving ocean models* Geophysical Monograph 177 (pp. 63–82). American Geophysical Union.

Leith, C. E. (1996). Stochastic models of chaotic systems. *Physica D*, *98*, 481–491.

Lemarié, F., Debreu, L., Shchepetkin, A. F., & McWilliams, J. C. (2012a). On the stability and accuracy of the harmonic and biharmonic isoneutral mixing operators in ocean models. *Ocean Modelling*, *52-53*, 9–35.

Lemarié, F., Kurian, J., Shchepetkin, A. F., Molemaker, M. J., Colas, F., & McWilliams, J. C. (2012b). Are there inescapable issues prohibiting the use of terrain-following coordinates in climate models? *Ocean Modelling*, *42*, 57–79.

Lique, C., Treguier, A.-M., Scheinert, M., & Penduff, T. (2009). A model-based study of ice and freshwater transport variability along both sides of Greenland. *Climate Dynamics*, *33*, 685–705.

Lombard, A., Garric, G., & Penduff, T. (2009). Regional patterns of observed sea level change: insights from a $1/4°$ global ocean/sea-ice hindcast. *Ocean Dynamics*, *59*, 433–449.

MacKinnon, J., Alford, M., Bouruet-Aubertot, P., Bindoff, N., Elipot, S., Gille, S., Girton, J., Gregg, M., Kunze, E., Naveira Garabato, A., Phillips, H., Pinkel, R., Polzin, K., Sanford, T., Simmons, H., & Speer, K. (2010). Using global arrays to investigate internal-waves and mixing. In J. Hall, D. Harrison, & D. Stammer (Eds.), *Proceedings of the OceanObs09 Conference: Sustained Ocean Observations and Information for Society, Venice, Italy, 21-25 September 2009*. ESA Publication WPP-306 volume 2.

Maltrud, M., & McClean, J. (2005). An eddy resolving global $1/10°$ ocean simulation. *Ocean Modelling*, *8*, 31–54.

Manizza, M., Le Quere, C., Watson, A., & Buitenhuis, E. (2005). Bio-optical feedbacks among phytoplankton, upper ocean physics and sea-ice in a global model. *Geophysical Research Letters*, *32*, doi:10.1029/2004GL020778.

Maqueda, M. M., & Holloway, G. (2006). Second-order moment advection scheme applied to Arctic Ocean simulation. *Ocean Modelling*, *14*, 197–221.

Marchesiello, J. M. P., Debreu, L., & Couvelard, X. (2009). Spurious diapycnal mixing in terrain-following coordinate models: The problem and a solution. *Ocean Modelling*, *26*, 156–169.

Marchesiello, P., McWilliams, J., & Shchepetkin, A. (2001). Open boundary conditions for long-term integration of regional oceanic models. *Ocean Modelling*, *3*, 1–20.

Margolin, L., Rider, W., & Grinstein, F. (2006). Modeling turbulent flow with implicit LES. *Journal of Turbulence*, *7*, 1–27.

Marsh, R. (2000). Cabbeling due to isopycnal mixing in isopycnic coordinate models. *Journal of Physical Oceanography*, *30*, 1757–1775.

Marshall, J., Adcroft, A., Campin, J.-M., Hill, C., & White, A. (2004). Atmosphere-ocean modeling exploiting fluid isomorphisms. *Monthly Weather Review*, *132*, 2882–2894.

Marshall, J., Hill, C., Perelman, L., & Adcroft, A. (1997). Hydrostatic, quasi-hydrostatic, and nonhydrostatic ocean modeling. *Journal of Geophysical Research*, *102*, 5733–5752.

Marshall, J., Jamous, D., & Nilsson, J. (1999). Reconciling thermodynamic and dynamic methods of computation of water-mass transformation rates. *Deep-Sea Research I*, *46*, 545–572.

Marshall, J., & Schott, F. (1999). Open-ocean convection: observations, theory, and models. *Reviews of Geophysics*, *37*, 1–64.

Martin, T., & Adcroft, A. (2010). Parameterizing the fresh-water flux from land ice to ocean with interactive icebergs in a coupled climate model. *Ocean Modelling*, *34*, 111–124.

Maze, G., Forget, G., Buckley, M., Marshall, J., & Cerovecki, I. (2009). Using transformation and formation maps to study the role of air-sea heat fluxes in the North Atlantic eighteen degree water formation. *Journal of Physical Oceanography*, *39*, 1818–1835.

McDougall, T. J. (1987). Thermobaricity, cabbeling, and water-mass conversion. *Journal of Geophysical Research*, *92*, 5448–5464.

McDougall, T. J. (2003). Potential enthalpy: a conservative oceanic variable for evaluating heat content and heat fluxes. *Journal of Physical Oceanography*, *33*, 945–963.

McDougall, T. J., Greatbatch, R., & Lu, Y. (2002). On conservation equations in oceanography: How accurate are Boussinesq ocean models? *Journal of Physical Oceanography*, *32*, 1574–1584.

McDougall, T. J., & McIntosh, P. C. (2001). The temporal-residual-mean velocity. Part II: isopycnal interpretation and the tracer and momentum equations. *Journal of Physical Oceanography*, *31*, 1222–1246.

McWilliams, J. C., Danabasoglu, G., & Gent, P. R. (1996). Tracer budgets in the warm water sphere. *Tellus Series A*, *48*, 179–192.

McWilliams, J. C., & Sullivan, P. (2001). Vertical mixing by Langmuir circulations. *Spill Science and Technology Bulletin*, *6*, 225–237.

Meehl, G., Covey, C., Delworth, T., Latif, M., McAvaney, B., Mitchell, J., Stouffer, R., & Taylor, K. (2007). The WCRP CMIP3 multimodel dataset: A new era in climate change research. *Bulletin of the American Meteorological Society*, *88*, 1383–1394.

Meehl, G., Gent, P. R., Arblaster, J., Otto-Bliesner, B., Brady, E., & Craig, A. (2001). Factors that affect the amplitude of El Niño in global coupled climate models. *Climate Dynamics*, *17*, 515–526.

Megann, A., New, A., Blaker, A., & Sinha, B. (2010). The sensitivity of a coupled climate model to its ocean component. *Journal of Climate*, *23*, 5126–5150.

Melet, A., Hallberg, R., Legg, S., & Polzin, K. (2013). Sensitivity of the Pacific Ocean state to the vertical distribution of internal-tide driven mixing. *Journal of Physical Oceanography*, (pp. doi:10.1175/JPO–D–12–055.1).

Melet, A., Verron, J., Gourdeau, L., & Koch-Larrouy, A. (2011). Solomon Sea water masses pathways to the equator and their modifications. *Journal of Physical Oceanography*, *41*, 810–826.

Mellor, G. L., Oey, L.-Y., & Ezer, T. (1998). Sigma coordinate pressure gradient errors and the seamount problem. *Journal of Atmospheric and Oceanic Technology*, *15*, 1122–1131.

Merryfield, W. J., & Scott, R. (2007). Bathymetric influence on mean currents in two high resolution near-global ocean models. *Ocean Modelling*, *16*, 76–94.

Mitrovica, J. X., Tamisiea, M. E., Davis, J. L., & Milne, G. A. (2001). Recent mass balance of polar ice sheets inferred from patterns of global sea-level change. *Nature*, *409*, 1026–1029.

Müller, P. (2006). *The Equations of Oceanic Motions*. (1st ed.). Cambridge: Cambridge University Press. 302pp.

Nakano, H., & Suginohara, N. (2002). Effects of bottom boundary layer parameterization on reproducing deep and bottom waters in a world ocean model. *Journal of Physical Oceanography*, *32*, 1209–1227.

Naveira-Garabato, A., Polzin, K., King, B., Heywood, K., & Visbeck, M. (2004). Widspread intense turbulent mixing in the Southern Ocean. *Science*, *303*, 210–213.

Olbers, D. J., Willebrand, J., & Eden, C. (2012). *Ocean Dynamics*. (1st ed.). Berlin, Germany: Springer. 704 pages.

Pacanowski, R. C. (1987). Effect of equatorial currents on surface stress. *Journal of Physical Oceanography*, *17*, 833–838.

Pacanowski, R. C., & Gnanadesikan, A. (1998). Transient response in a z-level ocean model that resolves topography with partial-cells. *Monthly Weather Review*, *126*, 3248–3270.

Palmer, T., & Williams, P. (2008). Stochastic physics and climate modelling. *Philosophical Transactins of the Royal Soceity A*, *366*, 2421–2427.

Palter, J. B., Griffies, S. M., Galbraith, E. D., Gnanadesikan, A., Samuels, B. L., & Klocker, A. (2013). The deep ocean buoyancy budget and its temporal variability. *Journal of Climate*, *submitted*.

Parkinson, C., & Washington, W. (1979). A large-scale numerical model of sea ice. *Journal of Geophysical Research*, *84*, 311–337.

Pedlosky, J. (1987). *Geophysical Fluid Dynamics*. (2nd ed.). Berlin Heidelberg New York: Springer-Verlag. 710 + xv pp.

Penduff, T., Juza, M., Brodeau, L., Smith, G. C., Barnier, B., Molines, J. M., Treguier, A. M., & Madec, G. (2010). Impact of global ocean model resolution on sea-level variability with emphasis on interannual time scales. *Ocean Science*, *6*, 269–284.

Penduff, T., Sommer, J. L., Barnier, B., Treguier, A.-M., Molines, J.-M., & Madec, G. (2007). Influence of numerical schemes on current-topography interactions in 1/4° global ocean simulations. *Ocean Science*, *3*, 509–524.

Philander, S. G. (1990). *El Niño, La Niña, and the Southern Oscillation*. Academic Press.

Polzin, K. L., Toole, J. M., Ledwell, J. R., & Schmitt, R. W. (1997). Spatial variability of turbulent mixing in the abyssal ocean. *Science*, *276*, 93–96.

Prather, M. (1986). Numerical advection by conservation of second-order moments. *Journal of Geophysical Research*, *91*, 6671–6681.

Price, J., & Yang, J. (1998). Marginal sea overows for climate simulations. In E. P. Chassignet, & J. Verron (Eds.), *Ocean Modeling and Parameterization* (pp. 155–170). Kluwer volume 516 of *NATO ASI Mathematical and Physical Sciences Series*.

Redi, M. H. (1982). Oceanic isopycnal mixing by coordinate rotation. *Journal of Physical Oceanography*, *12*, 1154–1158.

Redler, R., & Böning, C. W. (1997). Effect of the overflows on the circulation in the subpolar north atlantic: A regional model study. *Journal of Geophysical Research*, *102*, 18529–18552.

Reif, F. (1965). *Fundamentals of Statistical and Thermal Physics*. New York: McGraw-Hill.

Ringler, T., Petersen, M., Higdon, R. L., Jacobsen, D., Jones, P. W., & Maltrud, M. (2013). A multi-resolution approach to global ocean modeling. *Ocean Modelling*, ..., doi.org/10.1016/j.ocemod.2013.04.010.

Rivin, I., & Tziperman, E. (1997). Sensitivity of air-sea fluxes to SST perturbations. *Journal of Climate*, *11*, 2431–2446.

Roberts, M. J., & Marshall, D. (1998). Do we require adiabatic dissipation schemes in eddy-resolving ocean models? *Journal of Physical Oceanography*, *28*, 2050–2063.

Roberts, M. J., & Wood, R. (1997). Topographic sensitivity studies with a Bryan-Cox-type ocean model. *Journal of Physical Oceanography*, *27*, 823–836.

Rodgers, K., Blanke, B., Madec, G., Aumont, O., Ciais, P., & Dutay, J.-C. (2003). Extratropical sources of Equatorial Pacific upwelling in an OGCM. *Geophysical Research Letters*, *30*, doi:10.1029/2002GL016003.

Rosati, A., & Miyakoda, K. (1988). A general circulation model for upper ocean simulation. *Journal of Physical Oceanography*, *18*, 1601–1626.

Röske, F. (2006). A global heat and freshwater forcing dataset for ocean models. *Ocean Modelling*, *11*, 235–297.

Saunders, P., & King, B. (1995). Bottom currents derived from a shipborne ADCP on WOCE cruise A11 in the South Atlantic. *Journal of Physical Oceanography*, *25*, 329–347.

Schiller, A., & Fiedler, R. (2007). Explicit tidal forcing in an ocean general circulation model. *Geophysical Research Letters*, *34*.

Schmitt, R. W. (1994). Double diffusion in oceanography. *Annual Review of Fluid Mechanics*, *26*, 255–285.

Shchepetkin, A., & McWilliams, J. (2002). A method for computing horizontal pressure-gradient force in an ocean model with a non-aligned vertical coordinate. *Journal of Geophysical Research*, *108*, 35.1–35.34.

Shchepetkin, A., & McWilliams, J. (2005). The regional oceanic modeling system (ROMS): a split-explicit, free-surface, topography-following-coordinate oceanic model. *Ocean Modelling*, *9*, 347–404.

Shchepetkin, A. F., & McWilliams, J. C. (1998). Quasi-monotone advection schemes based on explicit locally adaptive dissipation. *Monthly Weather Review*, *126*, 1541–1580.

Simmons, H. L., Jayne, S. R., St.Laurent, L. C., & Weaver, A. J. (2004). Tidally driven mixing in a numerical model of the ocean general circulation. *Ocean Modelling*, *6*, 245–263.

Smagorinsky, J. (1993). Some historical remarks on the use of nonlinear viscosities. In B. Galperin, & S. A. Orszag (Eds.), *Large Eddy Simulation of Complex Engineering and Geophysical Flows* (pp. 3–36). Cambridge University Press.

Smith, K. S. (2007). The geography of linear baroclinic instability in earth's oceans. *Journal of Marine Research*, *65*, 655–683.

Smith, K. S., & Vallis, G. K. (2001). The scales and equilibration of midocean eddies: freely evolving flow. *Journal of Physical Oceanography*, *31*, 554–570.

Smith, R., Maltrud, M., Bryan, F., & Hecht, M. (2000). Numerical simulation of the North Atlantic at $1/10^{\circ}$. *Journal of Physical Oceanography*, *30*, 1532–1561.

Smith, R. D., & McWilliams, J. C. (2003). Anisotropic horizonal viscosity for ocean models. *Ocean Modelling*, *5*, 129–156.

Solomon, H. (1971). On the representation of isentropic mixing in ocean models. *Journal of Physical Oceanography*, *1*, 233–234.

Speer, K., & Tziperman, E. (1992). Rates of water mass formation in the North Atlantic Ocean. *Journal of Physical Oceanography*, *22*, 2444–2457.

Speich, S., Blanke, B., de Vries, P., Drijfhout, S., Döös, K., , Ganachaud, A., & Marsh, R. (2002). Tasman leakage: A new route in the global ocean conveyor belt. *Gophysical Research Letters*, *29*.

Stacey, M. W., Pond, S., & Nowak, Z. P. (1995). A numerical model of the circulation in Knight Inlet, British Columbia, Canada. *Journal of Physical Oceanography*, *25*, 1037–1062.

Stammer, D. (1998). On eddy characteristis, eddy transports, and mean flow properties. *Journal of Physical Oceanography*, *28*, 727–739.

Starr, V. P. (1945). A quasi-Lagrangian system of hydrodynamical equations. *Journal of Meteorology*, *2*, 227–237.

Stewart, A., & Dellar, P. (2011). The role of the complete Coriolis force in cross-equatorial flow of abyssal ocean currents. *Ocean Modelling*, *38*, 187 – 202.

Sullivan, P. P., & McWilliams, J. C. (2010). Dynamics of winds and currents coupled to surface waves. *Annual Review of Fluid Mechanics*, *42*, 19–42.

Sullivan, P. P., McWilliams, J. C., & Melville, W. K. (2007). Surface gravity wave effects in the oceanic boundary layer: large-eddy simulation with vortex force and stochastic breakers. *Journal of Fluid Mechanics*, *593*, 405–452.

Tatebe, H., & Hasumi, H. (2010). Formation mechanism of the Pacific equatorial thermocline revealed by a general circulation model with a high accuracy tracer advection scheme. *Ocean Modelling*, *35*, 245–252.

Taylor, P. (2000). Final Report of the Joint WCRP/SCOR Working Group on Air-Sea Fluxes: Intercomparison and validation of ocean-atmosphere energy flux fields. WCRP-112, WMO/TD-No.1036 (p. 303pp). World Climate Research Programme.

Timmermann, R., Danilov, S., Schröter, J., Böning, C., Sidorenko, D., & Rollenhagen, K. (2009). Ocean circulation and sea ice distribution in a finite element global sea ice-ocean model. *Ocean Modelling*, *27*, 114–129.

Toole, J. M., Schmitt, R. W., & Polzin, K. L. (1997). Near-boundary mixing above the flanks of a mid-latitude seamount. *Journal of Geophysical Research*, *102*, 947–959.

Treguier, A., Barnier, B., Miranda, A., Molines, J., Grima, N., Imbard, M., Madec, G., Messager, C., Reynaud, T., & Michel, S. (2001). An eddy-permitting model of the Atlantic circulation: Evaluating open boundary conditions. *Journal of Geophysical Research-oceans*, *106*, 22115–22129.

Treguier, A., Ferron, B., & Dussin, R. (2012). Buoyancy-driven currents in eddying ocean models. In E. Chassignet, C. Cenedese, & J. Verron (Eds.), *Buoyancy-Driven flows*. Cambridge UK: Cambridge University Press.

Treguier, A. M. (1992). Kinetic energy analysis of an eddy resolving, primitive equation model of the North Atlantic. *Journal of Geophysical Research*, *97*, 687–701.

Treguier, A. M., Le Sommer, J., Molines, J. M., & de Cuevas, B. (2010). Response of the Southern Ocean to the Southern Annular Mode: Interannual variability and multidecadal trend. *Journal of Physical Oceanography*, *40*, 1659–1668.

Tziperman, E. (1986). On the role of interior mixing and air-sea fluxes in determining the stratification and circulation in the oceans. *Journal of Physical Oceanography*, *16*, 680–693.

Vallis, G. K. (2006). *Atmospheric and Oceanic Fluid Dynamics: Fundamentals and Large-scale Circulation*. (1st ed.). Cambridge: Cambridge University Press. 745 + xxv pp.

van Sebille, E., Jan van Leeuwen, P., Biastoch, A., Barron, C. N., & de Ruijter, W. P. M. (2009). Lagrangian validation of numerical drifter trajectories using drifting buoys: Application to the Agulhas system. *Ocean Modelling*, *29*, 269–276.

Veneziani, M., Griffa, A., Garraffo, Z., & Chassignet, E. (2005). Lagrangian spin parameter and coherent structures from trajectories released in a high-resolution ocean model. *Journal of Marine Research*, *63*, 753–788.

Veronis, G. (1975). The role of models in tracer studies. In *Numerical Models of Ocean Circulation*. National Academy of Sciences.

Vialard, J., & Delecluse, P. (1998). An OGCM study for the TOGA decade. Part I: Role of salinity in the physics of the Western Pacific Fresh Pool. *Journal of Physical Oceanography*, *28*, 1071–1088.

Volkov, D., & Fu, L.-L. (2008). The role of vorticity fluxes in the dynamics of the Zapiola Anticyclone. *Journal of Geophysical Research*, *113*, C11015.

Vries, P., & Döös, K. (2001). Calculating Lagrangian trajectories using time-dependent velocity fields. *Journal of Atmospheric and Oceanic Technology*, *18*, 1092–1101.

Walin, G. (1982). On the relation between sea-surface heat flow and thermal circulation in the ocean. *Tellus*, *34*, 187–195.

Webb, D. (2000). Evidence for shallow zonal jets in the South Equatorial Current region of the Southwest Pacific. *Journal of Physical Oceanography*, *20*, 706–720.

Willebrand, J., Barnard, S., Barnier, B., Beckmann, A., Böning, C., Coulibaly, M., deCuevas, B., Dengg, J., Dieterich, C., Ernst, U., Herrmann, P., Jia, Y., Killworth, P., Kröger, J., Lee, M.-M., Provost, C., Molines, J., New, A., Oschlies, A., Reynaud, T., & West, L. (1997). *DYNAMO: Dynamics of North Atlantic Models: Simulation and assimilation with high resolution models*. available from hdl:10013/epic.10757: DYNAMO Scientific Report No 3.

Williams, P. (2005). Modelling climate change: the role of unresolved processes. *Philosophical Transactions of the Royal Society A*, *363*, 2931–2946.

Williams, R., Spall, M., & Marshall, J. (1995). Does Stommel's mixed layer 'demon' work? *Journal of Physical Oceanography*, *25*, 3089–3102.

Winton, M., Hallberg, R., & Gnanadesikan, A. (1998). Simulation of density-driven frictional downslope flow in z-coordinate ocean models. *Journal of Physical Oceanography*, *28*, 2163–2174.

Wirth, A., & Barnier, B. (2006). Tilted convective plumes in numerical experiments. *Ocean Modelling*, *12*, 101–111.

Wirth, A., & Barnier, B. (2008). Mean circulation and structures of tilted ocean deep convection. *Journal of Physical Oceanography*, *38*, 803–816.

Wu, W., Danabasoglu, G., & Large, W. (2007). On the effects of parameterized Mediterranean overflow on North Atlantic ocean circulation and climate. *Ocean Modelling*, *19*, 31–52.

Wunsch, C. (1997). The vertical partition of oceanic horizontal kinetic energy and the spectrum of global variability. *Journal of Physical Oceanography*, *27*, 1770–1794.

Wunsch, C., & Ferrari, R. (2004). Vertical mixing, energy, and the general circulation of the ocean. *Annual Reviews of Fluid Mechanics*, *36*, 281–314.

Wunsch, C., & Stammer, D. (1995). The global frequency-wavenumber spectrum of oceanic variability estimated from TOPEX/POSEIDON altimetric measurements. *Journal of Geophysical Research*, *100*, 24,895–24,910.

Xu, Y., & Scott, R. B. (2008). Subtleties in forcing eddy resolving ocean models with satellite wind data. *Ocean Modelling*, *20*, 240–251.

Young, W. R. (2012). An exact thickness-weighted average formulation of the Boussinesq equations. *Journal of Physical Oceanography*, *42*, 692–707.